Università
Ca'Foscari
Venezia

Master's Degree in Environmental Sciences

Final Thesis

Modeling potato crop yields for different agrophotovoltaic shading scenarios

Supervisor
Prof. Roberto PASTRES
Second Reader
Dr. Georg JÄGER

Graduand
Bianca UBERTI FOPPA
Matricolation number
975479

Academic Year 2021–2022

Abstract

The interest in agrivoltaic systems, which combine crops and electricity production in the same land, has increased in the last years especially thanks to the allocation of funds by the National Recovery and Resilience Plan (NRRP) in 2021 and the "Guidelines on agrivoltaic plants" in 2022, which state that such plants must not cause a reduction in the final crop yield.

For this reason, the objective of this thesis work is to evaluate the introduction of agrivoltaics in Italy through the study of the effect of the presence of photovoltaic panels on the final yield of a selected crop in a certain area, i.e. the potato crop in the area of Ferrara in the Emilia-Romagna region, to preliminary hypothesizing a first agrivoltaic configuration, in collaboration with A2A company.

The study of the impact of photovoltaic panels on the potato harvested yield was carried out by using the Decision Support System for Agrotechnology Transfer (DSSAT) software, which simulates more than 42 different crops under different spatial and temporal growth scenarios, considering several input parameters related to soil, meteorological and crop management data, which can be used as forcings depending on what is to be studied.

In the case of this thesis work, soil and crop management input parameters for the potato crop in the Ferrara area were estimated and validated to assess initial conditions. Subsequently, the crop yield for the years 2017-2022 was calculated using the crop model to understand the impact on crop yield of solar radiation, temperature, and precipitation, which were expected to change due to the presence of the panels.

As for the assessment of the initial conditions, the results confirmed the input data put as parameters thanks to the comparison between the simulated crop yield with that actually recorded in the area, which averaged 40 $t \cdot ha^{-1}$.

On the other hand, the annual variability analysis identified three categories of years based on the response to shading, i.e., where the yield decline occurred at 20% (2019), 30% (2017, 2020, 2022) and 40% (2018, 2021) shading, and based on the absolute yield of the crop, i.e., above average (2018), around average (2017, 2019, 2020) and below average (2021, 2022). These categories were useful for carrying out the study of the influence of individual meteorological parameters.

As for radiation, the results indicate that the monthly variability of radiation over the growing period does not present a definite pattern to explain the crop response to shading when considering individual months (with p-values below the significance threshold of 0.05), but becomes representative when considering the cumulative radiation of the first two to three months. This leads to the conclusion that there is an absolute value of incident radiation that must be reached in the first two months for the harvested yield to remain stable until the 30-40% shading scenario, within the range of (1223, 1301) $MJ \cdot sqm^{-1}$.

Furthermore, it was observed that this response to shading is influenced almost solely by radiation alone, while temperature and precipitation predominantly impact the absolute value of the crop yield in different years. Specifically for temperature, it was observed that an increase in temperature in suboptimal years (i.e. 2021 and 2022, as seen above) causes absolute crop yield to be comparable to the average of other years (with an average increase of 15-20%). This result is less evident when considering precipitation, for which an increase does not correspond automatically in an increase in absolute crop yield, especially in years with intermediate weather values, where the relationship between the three variables takes on a greater prevalence than the individual weather factors.

Finally, simulations were carried out for three agrivoltaic structures, which differed in row spacing (pitch), panel height, and panel configuration (1P or 2P, if the structure involves one or two attached panels). It was found that the 2P tracker structure with 14 m pitch is the optimal one, as the production drop occurs at 3.5 m distance from the panels, corresponding to 57% of the arable land not affected by the panels, with also a 10% increase in inter-row production compared to the scenario without panels.

In conclusion, the findings of this preliminary study indicate that agrivoltaic systems should be designed taking into account the need to ensure a minimum level of incident radiation at least in the first two months of cultivation, to avoid an inter-row production drop. Furthermore, photovoltaic panels are not responsible for the absolute low yield in years with unfavorable weather conditions, such as cold years; on the contrary, they may mitigate the damages to the crop by creating an underneath microclimate and the resulting higher temperature, which however is a hypothesis to be verified in more detail in future studies.

Index

Chapter 1

Introduction

Agrophotovoltaics, or agrivoltaic systems are designed to combine the production of photovoltaic electricity with crop soil agriculture, in order to increase the amount of electricity produced from renewable sources. Agrivoltaics, however, not only combines these two aspects of production, but is thought to ensure that crops benefit from the presence of photovoltaic panels, in some cases going so far as to increase crop yields.

Indeed, several studies in the literature indicate that certain types of crops are suitable for agrivoltaic application, taking advantage of the shading caused by photovoltaic panels as they are subject to less incident radiation. Among the earliest studies in this area, Beck et al. (2012) identify three different categories of plants based on their radiation requirements to carry out photosynthesis and grow: crops that benefit from some shading, crops that are not much influenced and crops that depend on maximum radiation and are not suitable for agrivoltaics. Potatoes, spinach and different types of salad were then classified as shade-tolerant. Other studies, however, consider more parameters beyond solar radiation, such as wind speed, air temperature, and humidity (Bellini, 2020) assuming the creation of a microclimate due to the presence of the panels, and always coming to identify leafy greens and root crops as the most suitable crops, especially in countries such as the United States, South Africa, and the Middle East. Indeed, as reported in more than one paper, geographic location greatly influences the adaptability of plants to agrivoltaic configurations, as for example observed in the experiment conducted by Adeh et al. (2019), in which they concluded that in regions with high solar potential, shading during specific growing periods and specific hours of the day were beneficial for vegetable crops such as potatoes (Kuruppuarachchi, 1990).

The above results indicate that agrivoltaics could be a very promising technology in a country like Italy, which is characterized by high solar exposure. However, to date, the implementation of agrivoltaics in Italy has not been thoroughly investigated, since the few studies on the topic focus on few crops, even if of interest for market deployment, such as soybean and wheat (Amaducci et al., 2018; Potenza, 2022).

Therefore, the objective of this thesis work is to evaluate the introduction of agrivoltaics in the Italian territory, meaning to study the impact of the presence of photovoltaic panels on the final

crop yields on the Italian soil, through the crop modeling software Decision Support System for Agrotechnology Transfer (DSSAT), which is in fact able to simulate 42 different crops in different spatial and temporal growth scenarios. To do this, a particular case study was selected, i.e. the one related to the potato crop, defined in the literature as particularly favorable for the application of agrivoltaics, in the area of Ferrara (Emilia-Romagna), an area that is orographically convenient for agrivoltaic deployment, as well as an area of greater spread of the crop itself.

The main research questions of the case study were therefore related to the effect of photovoltaic panels on the crop, i.e., the impact that the final crop yield has in response to lower incident radiation on the soil, and to the changes in the other two parameters affected by the presence of the panels due to the creation of an underlying microclimate, i.e., temperature and precipitation. This was done assuming that the crop is defined as suitable when the final harvested yield is not decreased significantly by the panels. Finally, thanks also to the collaboration with A2A, the second largest energy producer in Italy, the answers to the previous thesis questions were useful to hypothesize a first real agrivoltaic configuration that can be implemented in the Italian territory for the case study considered.

Therefore, the thesis retraces all the logical steps taken to answer the thesis questions. In Chapter 2 it starts from the context of the NRPP and the analysis of the "Guidelines on Agrivoltaic Plants" published by the Ministry of Ecological Transition in 2022 to frame the topic of agrivoltaics in the Italian regulatory context, and to define on which presented requirement to focus the analysis to assess the suitability of the crop for agrivoltaic application.

The choice of the crop and area of interest on which to evaluate the effect of the panels and address the resulting research questions is set forth in Chapter 3. The tool by which this study was addressed is subsequently presented in Chapter 4, in which the DSSAT software is explained in its general operation, with an indication of the main parameters and forcings to be considered. Always in this chapter, the DSSAT model specific to the selected crop is exposed, to understand how the variables of interest are described by it.

The parameters and forcings required by the model for the specific case of the selected crop and area are then described in detail in Chapter 5.

The presentation and discussion of the results of the case study are then set forth in Chapter 6. In particular, to answer the thesis question about the effect of photovoltaic panels on the growth of the potato crop, the analysis with DSSAT is carried out in several steps, first assessing the validity of the initial parameters found in Chapter 5, and then performing an annual analysis of the crop in order to understand the impact of variables such as radiation, temperature and rainfall, which are presumably subject to change due to the presence of the panels.

Finally, as above mentioned, this study leads to the final harvest of three agrivoltaic configurations hypothesized with the A2A company as potentially interesting for the study of agrivoltaic plants. The main discussions of this thesis are summarized in Chapter 7.

Chapter 2

Incentives and regulatory framework

2.1 National Recovery and Resilience Plan (NRRP)

Under the Next Generation EU program, a €750 billion investment and reform package to accelerate the green and digital transition in the wake of the pandemic crisis, Italy was the first beneficiary of two of the instruments made available by the European Union (Ministero dell'Economia e delle Finanze, 2021): the Recovery and Resilience Facility (RRF), with funding of €191 billion usable over the period 2021-2026, and the Recovery Assistance Package for Cohesion and the Territories of Europe (REACT-EU), consisting of about €37.5 billion to be used between 2021 and 2022 for the immediate revitalization of economies.

The resources allocated in relation to each country's GDP in 2019 saw Italy and Spain as the largest beneficiaries [Fig. 2.1].

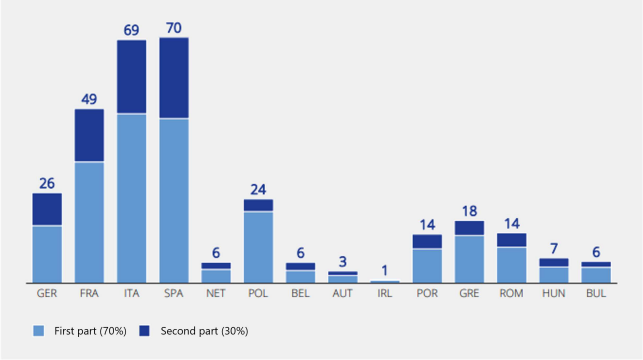

Figure 2.1: Grant allocation of the Recovery and Resilience Facility - RRF [€bn] (Italy's Recovery and Resilience Plan, 2021)

To benefit from this funding, Italy submitted an investment and reform plan in 2021, the National Recovery and Resilience Plan (NRRP), which includes six different missions:

1. Digitalization, Innovation, Competitiveness, Culture and Tourism
2. Green Revolution and Ecological Transition
3. Infrastructure for Sustainable Mobility
4. Education and Research
5. Inclusion and Cohesion
6. Health

The allocation of the €191.5 billion received from the EU was divided among the different missions, as shown in Fig. 2.2.

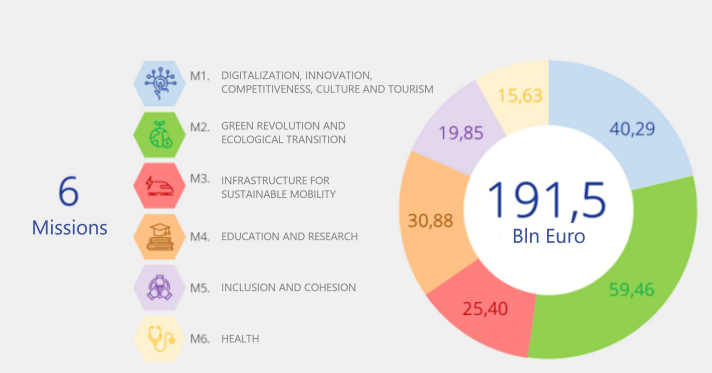

Figure 2.2: Grant allocation of the Recovery and Resilience Facility - RRF [€bn] (Italy's Recovery and Resilience Plan, 2021)

As the graph in Fig. 2.2 clearly shows, Mission 2, or "Green Revolution and Ecological Transition", is the one to which the most resources have been allocated, in line with the goals of the European Green Deal, a European program launched before the pandemic crisis to reduce greenhouse gases (GHG) emissions to 55% by 2030 and achieve climate neutrality by 2050.

For this reason, Mission 2 of the NRRP includes several types of objectives, such as: implementing actions for sustainable agriculture and improving waste management capacity, investing in renewable energy sources, developing the main supply chains toward ecological transition and sustainable mobility, as well as providing actions to improve the efficiency of the housing estate, combat hydrogeological disruption, safeguard biodiversity, and ensure the sustainable and efficient supply and management of water resources.

Under this mission, to initiate the progressive decarbonization of all productive sectors, the NRRP aims, among other measures, to increase the share of electricity generated from renewable sources, with centralized and decentralized solutions, also through smart agriculture and bioeconomy solutions. About €23.79 billion have been allocated for this purpose, divided into several sub-goals:

- Increase the share of energy produced from renewable sources: €5.9 billion
- Strengthen and digitize grid infrastructure: €4.11 billion
- Promote hydrogen production, distribution and end uses: €3.19 billion
- Develop more sustainable local transportation: €8.58 billion

- Develop international industrial and R&D leadership in key transition supply chains: €2.00 billion

Focusing on the first sub-target, which is to increase the share of energy produced from renewable sources, the goal for Italy is to cover about 30% of consumption by 2030. To achieve this goal, several strategic directions have been taken:

- Enable the unlocking of several utility-scale plants, including by focusing on the development of agrophotovoltaic plants.
- Increase the number of energy communities and distributed systems.
- Increase the development of innovative solutions, including offshore.
- Enhancing the development of biomethane.

For the purpose of this thesis work, only the first will be explored. The development of agrivoltaics, understood as a hybrid system of agriculture and photovoltaic power generation, defined in detail in the next section, has the dual objective of making the agricultural sector competitive and improving climate-environmental performance. Specifically, investment in the agrophotovoltaic sector aims to achieve a production capacity of 1.04 GW, equivalent to 1,300 GWh per year, with an estimated greenhouse gas reduction of about 0.8 million tons of CO_2 (Ministero dell'Economia e delle Finanze, 2021).

2.2 Guidelines on agrivoltaic plants

In June 2022, the document *Linee Guida in materia di Impianti Agrivoltaici* [Guidelines on Agrivoltaic Plants] was published by the Ministry of Ecological Transition, which establishes the requirements for defining a plant as agrivoltaic in order to access NRRP incentives.

The guidelines define agrivoltaic systems as "photovoltaic systems that allow the preservation of the continuity of agricultural and pastoral activities on the site of installation, while ensuring, at the same time, a good production of energy from renewable sources" (Ministero della Transizione Ecologica, 2022).

Specifically, an agrivoltaic system is defined as the total space occupied by photovoltaic modules, in configurations that allow for agricultural function, and the pore space, defined as the free space between and under the modules in which crops, soil, and crop structures are included. An agrivoltaic system can consist of one or more modules [Fig. 2.3], and the following definitions apply to each module.

Figure 2.3: Configurations of a single-module agrophotovoltaic system or a set of modules (Ministero Transizione Ecologica, 2022)

The technical requirements needed to define an agrivoltaic system are listed below and described in detail in the following subsections:

1. Integration between agriculture and photovoltaic (PV) production
2. Continuity of agricultural activity
3. Adoption of innovative solutions with modules elevated above the ground to optimize both thermal and agricultural performance.
4. Verification of impact on crops and recovery of soil fertility, microclimate and climate change resilience.

2.2.1 Integration between agriculture and PV production

There are two parameters that have been considered for an agrivoltaic system to be defined as integrated with that of electrical production:

1. *Minimum cultivated area*: minimum surface dedicated to cultivation ($S_{cultivated}$), established to be at least 70% of the total surface (S_{tot}), defined as the area used for crops and area on which the agrivoltaic system is located:

$$S_{cultivated} \geq 0.7 \cdot S_{tot} \tag{2.1}$$

2. *Maximum Land Area Occupation Ratio (LAOR)*: photovoltaic application density, thus the ratio of module area to agricultural area, which must have a maximum limit of 40%:

$$LAOR \leq 40\% \tag{2.2}$$

2.2.2 Continuity of agricultural activity

The elements defined in order not to compromise the continuity of agricultural and pastoral activity while ensuring efficient energy production are:

1. *Existence and yield of cultivation*: this data can be certified by considering the value of agricultural production on the area in the years following the agrivoltaic system [€/ha], and comparing it with that of previous years (or comparing it with a control area), with the same production address.
2. *Maintenance of production address*: it is necessary to maintain the same production address or switch to new address with higher economic value (CREA - Consiglio per la Ricerca in Agricoltura e l'analisi dell'Economia Agraria, 2021).
3. *Minimum electrical output*: the specific electrical production of an agrivoltaic system (named PV_{agri}) compared with the reference specific electrical output of a standard photovoltaic system (named $PV_{standard}$) must not be less than 60%:

$$PV_{agri} \geq 0.6 \cdot PV_{standard} \tag{2.3}$$

Both calculated in $GWh \cdot ha^{-1} \cdot yr^{-1}$.

2.2.3 Adoption of innovative agrivoltaic systems

The Guidelines place no restrictions on the structural characteristics of agrivoltaic systems, but list several types that can be built based on height, measured from the ground to the bottom edge of the photovoltaic module in the case of fixed structures, and to the maximum technically achievable tilt in the case of tracker structures. The types of structures are therefore:

1. *Type 1*: the minimum height of the modules allows agricultural or livestock activities even below the modules themselves, thus performing a synergies function to the crop, as of possible protection of the same.
2. *Type 2*: The minimum height does not allow activities to take place below the panels, but only activities between the rows. Thus there is simply a combined use of the soil.
3. *Type 3*: Modules in a vertical position, which does not affect the type of cultivable crop (except for shading), but decreases the degree of connectivity of the area

As a general guideline regarding the minimum height of modules, the Guidelines set 1.3 m in the case of livestock activities and 2.1 m in the case of crop activities.

2.2.4 Monitoring systems

Monitoring systems are required to evaluate the effectiveness of the measures above. Specifically, monitoring tools must be able to assess:

1. *Water savings through soil shading*, as well as the ability to collect and reuse stormwater through agrivoltaic structures.
2. *Continuity of agricultural activity*: i.e., the parameters listed in Section 2.2.2.
3. *Recovery of soil fertility.*
4. *Microclimate*: in fact, the presence of agrivoltaic structures may cause a change in the local microclimate that may affect the normal development of the plant; therefore, it is recommended to monitor several parameters, such as: temperature of the back-module and the external environment, humidity of the air in the back-module and the external environment, air velocity of the back-module and the external environment.
5. Resilience to climate change, both in the design phase and in the monitoring phase.

Thus, to answer the thesis question about the impact of photovoltaic panels on crops, as mentioned in the introduction, this thesis work focuses on studying the possibility for an agrivoltaic system to meet the requirement 1, specified in section 2.2.2, which is the requirement that the value of agricultural production [€/ha] has to be maintained on a given area in the years following the introduction of the agrivoltaic system, assuming that this means that the production yield, with the same crop, remains constant. This parameter is calculated by considering the total production of a given crop [kg/ha] and comparing the production data in the absence of photovoltaic panels with that corresponding to different shading scenarios due to the presence of the panels, taking as reference the potato crop in the Copparo area (Ferrara, Italy).

Chapter 3

Choice of the crop and the area

This chapter explains the choice of the crop on which the effects of photovoltaic panels were studied. In particular, the methodology for the identification of the crop on which to target the different research questions consisted in a literature research on the different experiments carried out around the world, particularly starting from the indications contained in the "Guidelines for Agrivoltaics Plants" and from the experiments carried out in locations with climatic conditions similar to those in Italy. On the other hand, after establishing potato as the target crop, the area on which to conduct the specific simulations was selected based on the crop's spread in terms of production per area.

3.1 Potato crop: previous experiments

The "Guidelines for Agrivoltaic Plants" (2022) indicate potatoes, hops, spinach, salads and broad beans as "very suitable crops" for agrivoltaics, taking up studies conducted on specific German spatial configurations and latitudes by the Fraunhofer Institute for Solar Energy Systems ISE (Agrivoltaics a Guideline for Germany, 2022). As these considerations are derived from the German climatic and technological situation, it is necessary to repeat the study of the impact of shading in the Italian context, but the German considerations can give a useful first indication of which crops to investigate in depth for Italian agrivoltaic application.

In the German experiments, tests were conducted in summer 2018 in Heggelbach, in the Bodensee-Oberschwaben region of southern Germany, on different crops such as winter wheat, potatoes, celery, and a mixture of grass and clover, grown under an agrivoltaic system with a height of 5 m (defined as the distance between the ground and the bottom edge of the panels) and a pitch of about 9 m (defined as the distance between two rows of panels).

As a result of the experiment, the land use efficiency for potatoes obtained as the summer of 2018 was particularly hot increased by about 86%, as shown in Fig. 3.1, demonstrating the potential of agrivoltaic in particularly hot and arid regions.

Figure 3.1: Potato growing increased land-use efficiency on the Heggelbach site to 186% (Agrivoltaics a Guideline for Germany, 2022)

This result can be explained by the potential of agrivoltaic to stabilize the crop yield particularly during dry periods due to its ability to shade crops and simultaneously reduce water consumption. However, the production capacity under the agrivoltaic system varied significantly when considering instead the previous production year, 2017, in which the reduction in yield due to shading was about 18-19% [Fig. 3.2]. This result suggests that for this crop, management at different growth stages may be necessary to avoid reaching a significant yield loss.

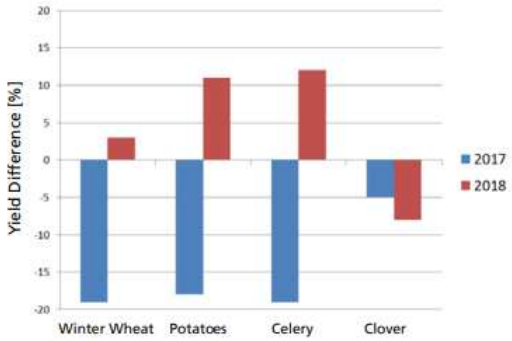

Figure 3.2: Crop yield differences under agrivoltaics compared to reference plots in Heggelbach in 2017 and 2018 (Agrivoltaics a Guideline for Germany, 2022)

In fact, the Fraunhofer Institute also suggests other crops for agrivoltaic application, as they are highly tolerant to shade, such as leafy vegetables (lettuce), field forage (grass and clover mixture), and various types of pome and stone fruits, berries, berries, and other specialty crops.

Other studies conducted on potato under climatic conditions in southwestern Germany (Schulz, 2019) analyzed the effects of shade on growth, yield, and quality when subjected to different levels of artificial shading (12%, 26%, and 50%), obtaining significant changes in growth at 50% shade, as seen in Fig. 3.3.

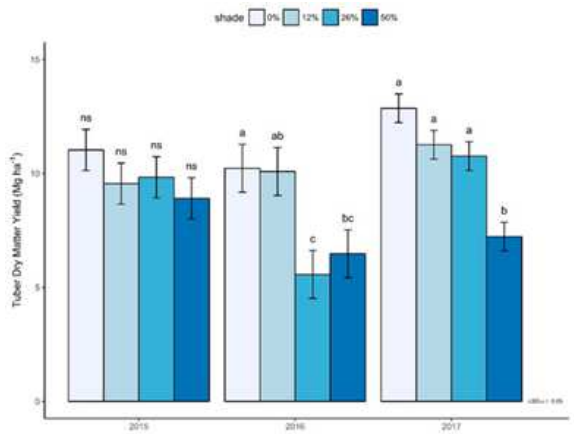

Figure 3.3: Tuber Dry Matter yield ($Mg \cdot ha^{-1}$) for different shading scenarios (0%, 12%, 26% and 50%) in three years (Schulz, 2019)

This study also indicates the average total irradiation for different irradiation scenarios to reach the light saturation point of 400 $\mu mol\ m^{-2}\ s^{-1}$ of Photosynthetic Active Radiation (PAR) to maximize yields, depicting them in a map of Europe [Fig. 3.4]. The average total irradiation thus corresponds to 16.89 MJ $m^{-2}day^{-1}$ for 12% shading, 20.08 MJ $m^{-2}day^{-1}$ for 26% shading, and 29.72 MJ $m^{-2}day^{-1}$ for 50% shading.

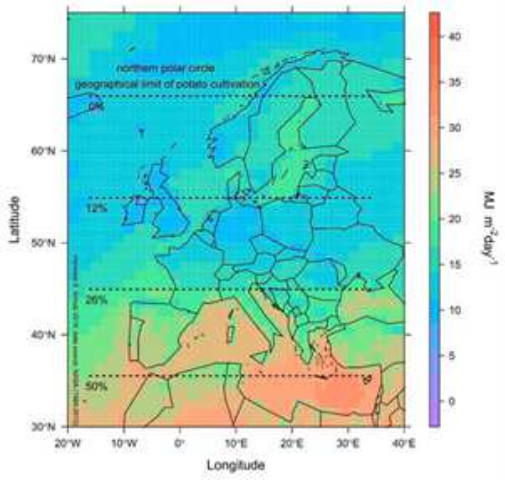

Figure 3.4: Solar irradiance during the potato growing season in Europe (MJ $m^{-2}\ day^{-1}$) (Schulz, 2019)

As can be seen from Fig. 3.4, Italy has average favorable solar conditions, which is why it is interesting to test the hypothesis of potato cultivation under agrivoltaic configurations in this thesis work.

3.2 The area selection

As previously mentioned, the area on which to conduct the specific simulations was selected based on the crop's spread.

According to the *7° Censimento generale dell'Agricoltura 2021* [7^{th} General Census of Agriculture 2021] by the National Institute of Statistics (ISTAT, 2021), which collects the main indicators of the agricultural sector every ten years, Emilia-Romagna has the largest cultivated area for potatoes of all other Italian regions, with about 5,000 ha available in the years 2020-2022.

Moreover, again according to ISTAT data (2021), as shown in Table 3.1, Ferrara ranks second among Emilia-Romagna provinces in 2021 in terms of cultivated area and quantity of production of the tuber.

Table 3.1: Area used for potato cultivation and quantity harvested by province in Emilia-Romagna (ISTAT, 2021).

Province	Total area $[ha]$	Total production $[q]$	Production per area $[q/ha]$
Bologna	2,042	802,920	393.2
Ferrara	1,350	661,500	490.0
Ravenna	880	440,000	500.0
Rimini	158	47,400	300.0
Forlì Cesena	152	62,340	410.1
Piacenza	61	11,940	195.7
Parma	45	5,120	113.8
Reggio nell'Emilia	41	8,015	195.5

In particular, if production is considered in relation to the cultivated area, it can be seen that Ferrara is the second province immediately after Ravenna, with about 490 $q \cdot ha^{-1}$. This value is in line with the indications of the Emilia-Romagna Region (Disciplinari Di Produzione Integrata - Norme Tecniche per Le Colture Orticole - Patata, 2022), which indicates average potato production per hectare over the years between 40 and 55 $t \cdot ha^{-1}$.

This fact, combined with the lowland orography of the area that would facilitate the testing and construction of agrivoltaic plants, makes it the target province on which to focus the thesis work.

Chapter 4

DSSAT

As stated in the introduction, the free software Decision Support System for Agrotechnology Transfer (DSSAT) was selected to study the effect of photovoltaic panels on the potato crop in the Ferrara area. This chapter will then give an overview of the general operation of DSSAT, highlighting the input parameters and the forcings it requires, and then detail the SUBSTOR-potato model present in DSSAT to simulate the growth of the potato crop, in order to highlight how the main meteorological forcings affect the growth of the crop according to the model.

4.1 Overview

The Decision Support System for Agrotechnology Transfer (DSSAT) software is a free software application program that simulates more than 42 different crops under different spatial and temporal growth scenarios, thanks to a rich database of soil types, weather and crop management (DSSAT Overview, 2022). The software was first released in 1989 by a team of scientists from the International Benchmark Sites Network for Agrotechnological Transfer (IBSNAT), a network established by the University of Hawaii that became part of the U.S. Agency for International Development (USAID) program, and which since 1994 has evolved into an International Consortium for the Application of Agricultural Systems (ICAAS), composed of former members of the IBSNAT network, scientists from Wageningen Agricultural University and the Agricultural Production Systems Research Unit in Australia (Hoogenboom et al., 2010). DSSAT has thus been used over the years by more than 25,000 researchers, policy and decision makers in more than 183 countries around the world, up to the latest version released (v.8) in 2021.

Among the various possible applications to be highlighted, DSSAT has been used to simulate the impact of climate change on agricultural and natural ecosystems, subsequently utilized in the Intergovernmental Panel on Climate Change (IPCC) assessments for agriculture (Reilly, 1996).

As above mentioned, in the specific case of this thesis work, DSSAT will be used to simulate different shading scenarios by modifying the environmental input data, particularly that of radi-

ation intensity, which is assumed to vary due to the presence of photovoltaic modules, as well as temperature and precipitation.

For this purpose, DSSAT is structured with a modular approach [Fig. 4.1], which is based on a Crop System Model (CSM) that encapsulates models for more than 42 different crops, considering weather, genetics, soil water, soil carbon and nitrogen in one or more seasons in any geographic location as input data.

As described in Fig 4.1, each "primary module" has six steps that must be performed for its use, controlled by the main program: run initialization, season initialization, rate calculation, integration, daily output, and summary output. These steps allow the state variables of each model to be read and integrated totally independently, thus allowing them to be replaced if there are changes in the simulation. This is done by means of a dynamic variable at the beginning of the simulation, and then retrieving the input modules, the land and crop file to create a temporary file that can be used by subsequent modules. The land unit module is then called up to initialize it (Hoogenboom et al., 2010).

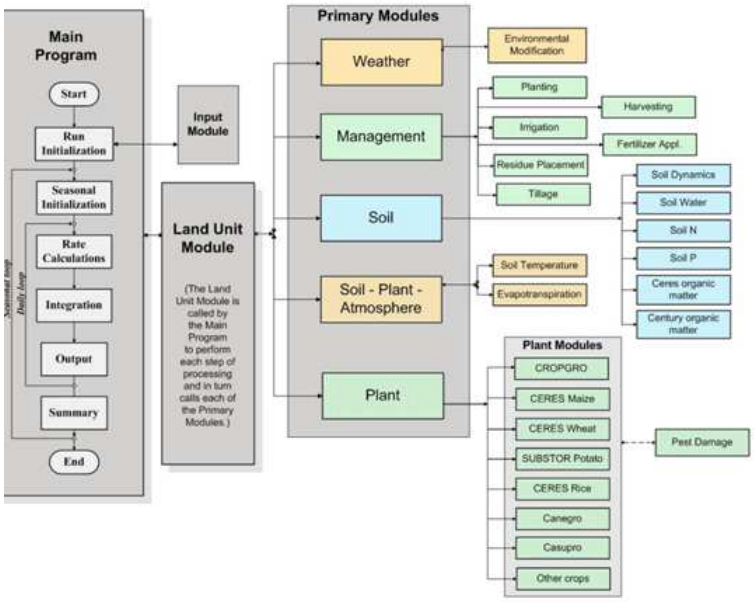

Figure 4.1: Overview of the components and modular structure of the DSSAT – CSM (Model Components, 2020)

Moreover, each primary module has submodules, which are described in the last column on the right of Fig. 4.1. Let us analyze each primary module in detail:

1. *Weather module*: it has the primary function of reading daily weather data (such as minimum and maximum air temperature, solar radiation, precipitation, wind speed, relative humidity) and generating missing ones.
2. *Soil module*: it contains information related to:
    - Soil water: to change the water content in the soil due to rainfall and irrigation, evaporation, water content absorbed by roots.

- Soil temperature: calculated from air temperature, also takes into account the impact of solar radiation and albedo on surface temperature.
- Carbon and nitrogen in the soil: the model simulates the presence of organic matter, distinguishing it into three types based on composition, and the nitrogen balance in the soil.
- Soil dynamics: reads soil parameters and changes them according to different parameters, such as tillage or changes in carbon presence over the long term.

3. *Soil-plant-atmosphere module*: this is the module used to calculate daily soil evaporation and plant transpiration, taking into account soil, plant and atmospheric inputs.
4. *Plant module*: this module was developed with an extremely generic approach, that allows the prediction of the growth of a different number of crops. However, the models that describe the crops are different, because some are based on the CROPGRO model (which describes several legumes, such as soybeans, peanuts, dry beans, and some non-legumes, such as tomatoes, cabbage, etc.), while others are models that individually describe some crops. Generic parameters used by this module for different types of crops include photosynthesis, respiration, nitrogen fixation parameters, plant growth parameters, and so forth. For each species, these parameters are defined at baseline and optimum temperature and are used at all stages of crop development (rate of emergence, rate of leaf emergence, rate of progress to flowering and maturity) and growth. Among these models, there is also the SUBSTOR-potato module, which describes the growth of the potato crop, discussed in detail in the following section.
5. *Management module*: it includes all those operations such as planting, harvesting, fertilization, irrigation, and application of crop residues or organic material, which can be specified directly by the end user, either automatically or fixed.

Therefore, as just noted, DSSAT has numerous state variables, forcings, parameters and outputs. Those of interest in answering the research questions of this thesis work are summarized in Tab. 4.1, at the end of the chapter.

The parameters in Tab. 4.1 will be used to identify several representative samplings of the Copparo area on which to perform the simulations. Of these samplings, only one will be used to carry out the simulations regarding the effect of the presence of photovoltaic panels on the crop, thus varying only the forcings according to the research question addressed and obtaining the corresponding crop yield. In particular, the variation of crop yield as radiation, temperature and precipitation change will be analyzed in detail in Chapter 5.

4.2 The SUBSTOR-potato model

As shown in Section 4.1, DSSAT contains within it several models to simulate different types of crops. Among them, the SUBSTOR model (Hoogenboom et al., 2010) describes the biomass accumulation and partitioning and phenomenological development of the potato crop (*Solanum tuberosum L.*), taking into consideration mainly three factors, such as:

- *Temperature* (mainly the daily minimum temperature)
- *Photoperiod or length of day*
- *Intercepted radiation*

In addition, the SUBSTOR-potato model also uses data such as water and nitrogen dynamics in the soil.

However, only the three listed variables and the equations used to describe the dependence of potato growth on them will be analyzed in this section.

4.2.1 Relative temperature equations

The functions used to describe the dependence of potato crop on temperature are mainly based on two components: daily average air temperature and soil temperature.

These two variables are in fact used to describe:

- *RTFVINE* (Relative Temperature Factor, for vine growth): leaf growth and vegetative biomass accumulation.
- *RFTSOIL* (Relative Temperature Factor, for tuber & root growth): it is used for seed, root and tuber growth stages.

According to the following equations:

$$\begin{aligned} RTFSOIL &= 0 && \text{if } ST \leq 2 \text{ or } ST > 33 \\ &= 0.079 \cdot (ST - 2) && \text{if } 2 < ST \leq 15 \\ &= 1 && \text{if } 15 < ST \leq 23 \\ &= 1 - 0.1 \cdot (ST - 23) && \text{if } 23 < ST \leq 33 \end{aligned} \tag{4.1}$$

where ST is the mean daily Soil Temperature, calculated in °C.

$$\begin{aligned} RTFVINE &= 0 && \text{if } XT \leq 2 \text{ or } XT > 35 \\ &= 0.0667 \cdot (XT - 2) && \text{if } 2 < XT \leq 17 \\ &= 1 && \text{if } 17 < XT \leq 24 \\ &= 1 - 0.909 \cdot (XT - 24) && \text{if } 24 < XT \leq 35 \end{aligned} \tag{4.2}$$

where XT is the mean daily air temperature, calculated in °C. These equations are represented graphically as in Fig. 4.2.

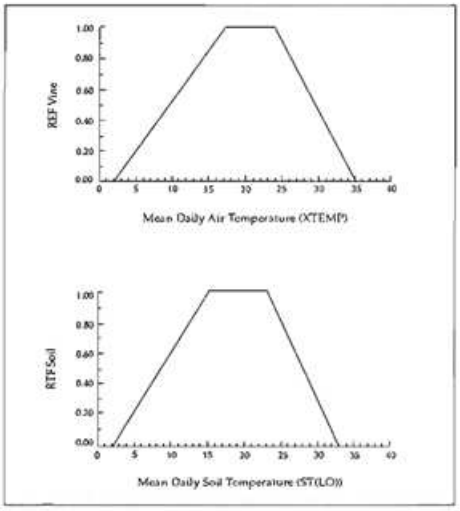

Figure 4.2: Mean Daily Air Temperature and Mean Daily Soil Temperature functions for leaf growth and tubers growth

It is clear from these equations that the leaves, tuber, and potato roots have different temperature response functions and that they have an optimal temperature range for the development of both. This range will be taken into account to analyze the results of the simulations in the following chapters.

4.2.2 Phenological development - Photoperiod and temperature

The phenological growth of potato can be described in five developmental stages. These developmental stages described by the model are:

1. Pre-plant
2. From planting to shoot germination
3. Shoot budding to emergence
4. From emergence to tuber initiation
5. Tuber initiation to maturity

The initiation or inhibition of potato growth, in particular, is a function of temperature and photoperiod, which is also influenced by the amount of nitrogen and water in the soil.

In particular, the dependence of crop growth inhibition can be described with different hypotheses, considering both variables. Regarding temperature, the assumptions to be considered are:

- Crops vary greatly in the temperature above which tuber initiation is inhibited.
- Tuber initiation is influenced much more by daily minimum temperature than by average or maximum temperature.

To simulate the effect of high temperatures on tuber initiation, the model uses a Relative Temperature Factor for Tuber Initiation (RTFTI), similar to the RTFVINE function. Each crop is

assigned a critical temperature (TC) above which the tuber is inhibited.

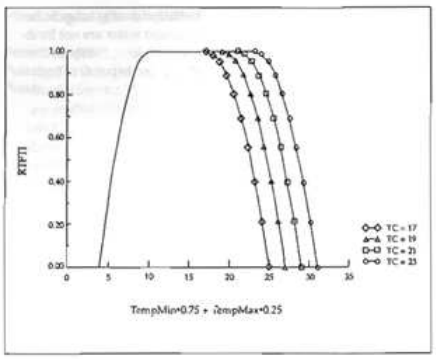

Figure 4.3: Relative thermal time function for effect of relative temperature factor for tuber initiation (RTFTI) (Hoogenboom, 2010)

Therefore, an optimal temperature range in which tuber growth is maximal was also observed for this plant [Fig. 4.3]. This range will be taken into account for subsequent analysis.

As for the effect of the Relative Daylength Factor for Tuber Initiation (RDLFTI), instead, in this case it is described by the following assumptions:

- If the photoperiod is less than 12 hours, RDLFTI is equal to 1 for all crops, i.e., crops develop tubers at about the same time under favorable (i.e., short) photoperiods. Differences between crops appear when photoperiods are long (and thus temperatures high).
- Photoperiod longer than 12 hours: early cultivars are less sensitive than late cultivars. Each cultivar is assigned a genetic coefficient P2 (0.2 to 0.8).

Therefore, the situation is represented as follows [Fig. 4.4]:

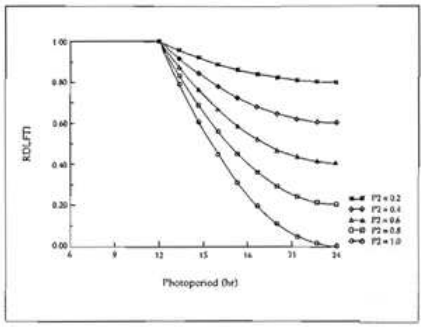

Figure 4.4: Function for relative effect of photoperiod on tuber initiation (RDLFTI) (Hoogenboom, 2010)

This function states that for long periods of photoperiod and high temperatures, tuber inhibition is high. This condition will not be given special consideration because the model does not allow for hourly variations in environmental conditions, which are in fact calculated automatically by DSSAT.

4.2.3 Biomass Accumulation – Intercepted radiation

The third variable of interest describing potato growth in the SUBSTOR-potato model is intercepted radiation, which is critical for photosynthetic assimilation, especially in the vegetative stage of development. Specifically, current photosynthetic assimilation is calculated as Potential CARBon assimilation of photosynthetic C (PCARB $[g \cdot plant^{-1} \cdot day^{-1}]$), a function of:

$$PCARB = 3.5 \cdot PAR/PLANTS \cdot (1.0 \cdot EXP(-0.55 \cdot LAI)) \tag{4.3}$$

where PAR is the Photosynthetic Active Radiation, which is the amount of radiation between 400 and 800 nm that each plant absorbs to carry out photosynthesis differently depending on the type of plant, and LAI is the Leaf Area Index.

The carbohydrate reserve that the plant absorbs (CARBO $[g \cdot plant^{-1} \cdot day^{-1}]$) is then calculated assuming that soil nutrients and water are not limiting, otherwise it is calculated as it follows:

$$CARBO = PCARB \cdot min(TM, SM, NM) + 0.5 \cdot CLF \tag{4.4}$$

where TM, SM and NM are unitless modifiers respectively for temperature, soil water and N stress effects on photosynthetic efficiency, and CLF is the amount of photosynthesis transferred in leaves before the abscission phase.

At later stages of development, such as tuber enlargement, Radiation Utilization Efficiency (RUE) can increase up to 50% or more as tubers accelerate photosynthetic assimilation more. To simulate this phenomenon, the model uses PCARB, increasing PAR to 4.0 $g \cdot MJ^{-1}$ to simulate the increase in RUE. The effective carbon assimilation (CARBO) is calculated as above.

Finally, this model, as mentioned earlier, takes into account some stressors such as the soil water deficit factor, which goes to affect expansion growth and photosynthetic rates, and the nitrogen deficit factor. However, these factors will be analyzed not directly in the simulations in this thesis work, which will focus on crop response to parameters such as radiation, temperature and precipitation.

Table 4.1: Input and output data required by DSSAT

Input data			
Category	Type	Variable name	Unit
Meteorological data	Forcing	Daylength	h
		Daily average global radiation	$MJ \cdot m^{-2} \cdot day^{-1}$
		Maximum daily temperature at 2m	°C
		Minimum daily temperature at 2m	°C
		Daily cumulative precipitation	mm
		Average daily relative humidity at 2 m	%
		CO_2	vpm
Soil data	Parameter	Sand, silt and clay	%
		pH in water	-
		Organic matter	%
		K_2O assimilable	mg/kg
		P_2O_5 assimilable	mg/kg
		Total N	%
		Lower limit	-
		Drained upper limit	-
		Saturated water content	-
		Saturated hydraulic content (Ksat)	cm/h
		Runoff curve number	-
		Runoff rate	mm/h
		Albedo	-
Crop management data	Parameter	Crop species	-
		Planting date	-
		Population density	$plants/m^2$
		Row spacing and planting depth	cm
		Irrigation thresholds	%
		Fertilizer type	-
		Fertilizer depth	cm
		Fertilizer quantity	kg/ha
		Tillage depth	cm
		Chemical quantity	l/ha
		Harvest date	-
Output data			
-	-	Harvested yield	$kg[dm]/ha$

Chapter 5

Input data: parameters and forcings

As seen in Chapter 4, DSSAT is structured into several modules, each of which requires different input data. Therefore, this chapter will analyze the input data to carry out simulations of different shading scenarios due to the presence of photovoltaic panels on the potato crop. These data are divided into: metereological data, soil data, and management data as forcings and parameter data.

5.1 Forcings: meteorological data

The years considered for the different potato harvest simulations range from 2017 to 2022. This was done in order to have a meaningful historical series that nevertheless took into account as little as possible the change in final harvest due to the increase in average temperatures globally caused by climate change, which to date stands at about 1°C compared to the pre-industrial period (Intergovernmental Panel on Climate Change, 2018), as it is not directly studied in this thesis work. Considering the last six years, it was therefore assumed to observe a change in weather data mainly due to weather variability in different years, thus being able to draw conclusions that can then be extended to any subsequent studies related to the influence of climate change on harvest in agrivoltaic fields.

Meteorological data were then extracted from the Hourly And Daily Weather Dataset (ERG5 - Dataset Meteo Orario E Giornaliero Dal 2001 - Dati Arpae, n.d.) from the *Osservatorio Clima, dall'Unità Territorio e dalle reti di Arpae Simc*. These data cover the entire territory of the Emilia-Romagna Region from 2001 to the present, through the spatial interpolation of values measured by the different meteorological stations on the territory, such as air temperature, precipitation, relative humidity, intensity (scalar and vector) and wind direction, and solar irradiance.

In order to obtain reliable data for each of these variables even in areas not directly sampled due to the absence of meteorological stations, several quality control procedures were carried out by Antolini et. al (2015), such as: elimination of spurious data, time homogeneity check between time series, time synchrony check on diurnal time scale (these three performed once), consistency check

of variables, and spatial check. In particular, the latter procedure was performed by assuming that the values of the variables remained constant in an unsampled area surrounding the area with the presence of meteorological stations, while taking into account orographic diversity and its impact on the variables considered. The territory of Emilia-Romagna was then divided with a grid based on these data [Fig. 5.1].

Figure 5.1: Graphical interface for downloading ERG5 data by cell and year - Emilia-Romagna (Geoportale, n.d.)

The values of interest were extracted by taking as a spatial reference the Copparo area identified by the grid square in Fig. 5.1, and considering, as mentioned above, the years 2017-2022.

Specifically, in this thesis work, some of the values available in the regional database were considered. These include:

- Daily average global radiation [MJ/m^2]
- Daily minimum and maximum temperature at 2 m [°C]
- Daily cumulative precipitation [mm]
- Average daily relative humidity at 2 m [%].

Finally, in order to further reduce the meteorological variability of the different years considered, a climatology of these years was also carried out, i.e., all daily values of the years 2017-2022 were averaged to obtain a reference year, taken as an average meteorological year.

5.2 Parameters: soil data

5.2.1 Chemical and physical sampling and parameters

Soil samples from the Ferrara area, and more specifically from the Copparo area, were extracted from the official 3D map viewer of the Emilia-Romagna Region for web consultation of GIS data (Geoportale 3D, n.d.). In particular, these values belong to the dataset *Campioni di Analisi del Territorio* [Land Analysis Samples] (Servizio di Analisi e Consulenza del Territorio - SACT) of

the Emilia-Romagna Region (Tarocco, 2021). The SACT, indeed, is an organization established in 1979 by the collaboration between the Agricultural Development Service of the Department of Agriculture of the Emilia-Romagna Region and the Professional Organizations of Agricultural Cooperatives, with the aim, among others, of creating a pedological database of the Emilia-Romagna Region through various samplings carried out over the years [Fig. 5.2].

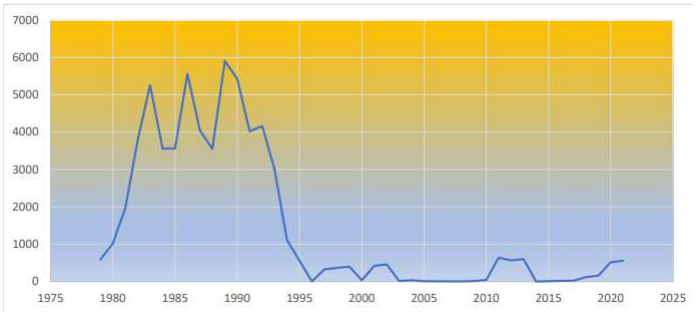

Figure 5.2: Number of Emilia-Romagna soil samples analyzed in the years by SACT [1979-2021] (Tarocco, 2021)

As shown in Fig. 5.2, most of the surveys were carried out in the decade 1980-1990, and can still be considered valid because soils have relatively constant characteristics over time (Ministero dell'Agricoltura e delle Foreste, 1998), especially basic soil characteristics such as texture, pH, total calcium carbonate. On the other hand, for other characteristics, such as analyses of assimilable phosphorus and exchangeable elements in areas where fertilization interventions are taking place, it is necessary to repeat sampling every five years (The Interpretation Of Soil Analyses, n.d.). Therefore, the values considered for this thesis work refer to the last decade of sampling.

Of the 62,053 samples gathered by SACT, 81.3% were in lowland areas, 12.3% in hilly areas, and 6.4% in mountainous areas, as seen in Fig. 5.3. To obtain these data, two survey campaigns were carried out: the first between 1999 and 2013 and the second between 2018 and 2023, the latter for areas that were poorly sampled or had sampled too old (Tarocco, 2021).

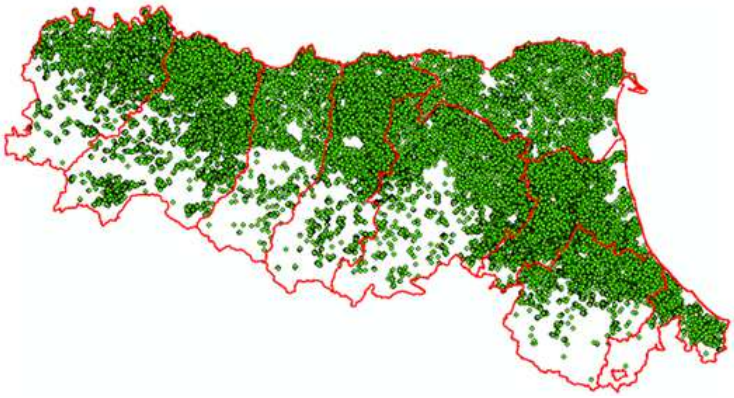

Figure 5.3: Distribution of the 62,053 samples in the SACT dataset (Tarocco, 2021)

Sampling was also done in a composite manner, that is, selecting different plots to represent greater agronomic variability, and selecting the surface layer (within 60 cm), although for the provinces of Ferrara and Ravenna sampling was sometimes done at more significant depths.

Thus, the chemical and physical analysis data available for each sampling are:

- Year of sampling
- Depth of sampling [m]
- Sand [%]
- Silt [%]
- Clay [%]
- pH in water
- Total limestone [%]
- Active limestone [%]
- Organic matter [%]
- K_2O assimilable [mg/kg]
- P_2O_5 assimilable [mg/kg]
- Total N (per thousand) [%]

However, only some of these data are required by the DSSAT software to characterize the soil on which the simulation is to be carried out, either to define its texture and the most stable parameters over time, or to indicate the initial analysis conditions in a given year through the least durable of the parameters listed above (such as K_2O assimilable, P_2O_5 assimilable, total N, pH in water, organic matter).

Seven different samplings were then considered for the Copparo area (Geoportale 3D, n.d.) [Fig. 5.4], classified on the map according to the percentage of clay in each.

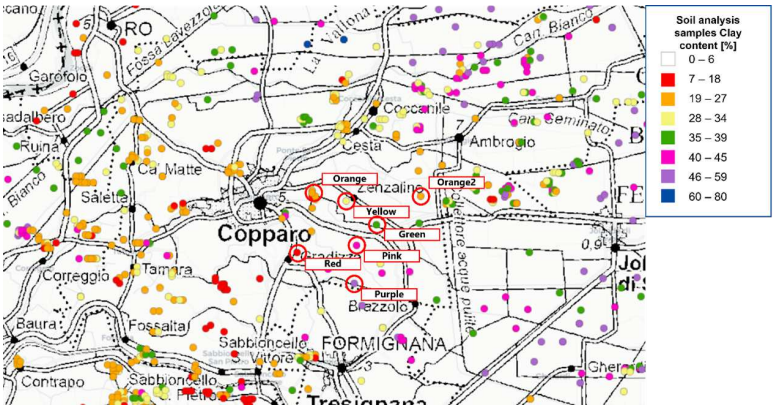

Figure 5.4: Selected samples in the Copparo area (3D Geoportale, n.d.)

The samplings considered in the Copparo area were selected in a perimeter of limited extent based on the assumption that although they still differ in percentage of clay, sand, and silt, the other soil parameters may differ less significantly, and thus not constitute a parameter of variability in the simulations.

Additional parameters required by DSSAT were derived for each of these samplings, such as: texture, soil water retention capacity (defined by lower boundary, drained upper boundary, and satu-

rated water content), runoff curve number, bulk density, saturated hydraulic conduction, albedo, drainage rate.

5.2.2 Soil texture

Soil texture is one of the most widely used characteristics for describing soils and refers to the weight of the fraction of sand, silt and clay present in the soil (Owens & Rutledge, 2005), which is important for understanding soil response to the presence or addition of water.

Several textural classification systems exist, among which one of the most widely used is the United States Department of Agriculture (USDA) soil texture triangle (Russell & Paris, 1986) [Fig. 5.5]: by drawing straight lines parallel to the sides of the triangle at the percentages of sand, silt and clay in the soil, its texture can be identified at the intersection of the three lines. This classification can also be derived using the automated online calculator, the USDA Soil Texture Calculator (U.S. Department of Agriculture, n.d.).

Figure 5.5: Soil texture triangle (Groenendyk et al., 2015)

Therefore, the DSSAT software requires the percentages of sand, silt and clay in the soil as primary data for soil definition. However, texture is a variable parameter when considering a fairly large area such as Copparo, as observed from Fig. 5.6.

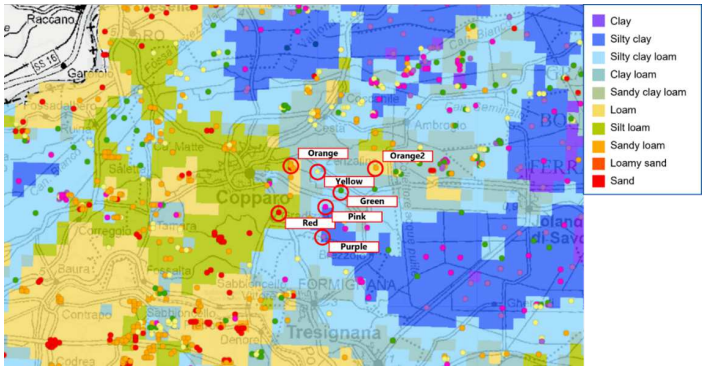

Figure 5.6: Text classification of the Copparo area (Geoportale 3D, n.d.)

Indeed, soils in the Copparo area have textures ranging from silt loam, to silty clay loam to silty clay to loam. The map in Fig. 5.6, when superimposed on the land-use vector cover map [Fig. 5.7] (Geoportale 3D, n.d.), brings out how most of the arable land, horticultural crops, orchards and in general crops in the area are cultivated indiscriminately in the four different textures.

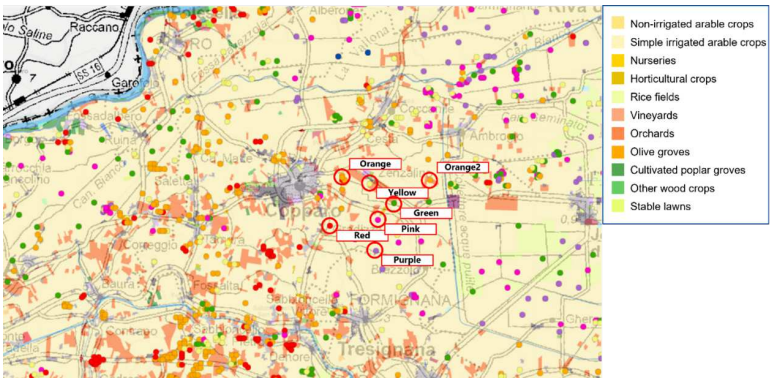

Figure 5.7: Vector land use coverages of the Copparo area (Geoportale 3D, n.d.)

All textures were then considered for different simulations of potato cultivation under different shading scenarios.

5.2.3 Soil water balance

In addition to values derived from chemical analyses of soil samples, DSSAT requires water parameters that define the soil water balance, that being the amount of water from irrigation or precipitation that is absorbed or not absorbed based on the surface, hydrological, and water content characteristics of the soil. These dynamics are governed by the potential differences in each soil horizon, defined by the points of potential lower boundary, drained upper boundary and saturated water content (Antolini et al., 2015).

Lower limit, drained upper limit e saturated water content

The lower limit is defined as the threshold below which it becomes impossible for plants to extract water at a rate that meets their water needs (Datta et al., 2017). For this reason, this threshold is also referred to as the wilting point, since near this value all vital processes of the plant stop, causing a significant reduction in growth and final yield.

The drained upper limit, on the other hand, is the maximum amount of water that can be retained by the soil once water is removed by gravitational force at the end of rapid drainage, after the soil has become saturated (Water Reserve, n.d.). This quantity is also called Field Capacity (FC).

Finally, saturated water content is the threshold at which all soil pores are filled with water, which is why it is called maximum water capacity (Antolini et al., 2015).

The three potential points can then be represented as in Fig. 5.8.

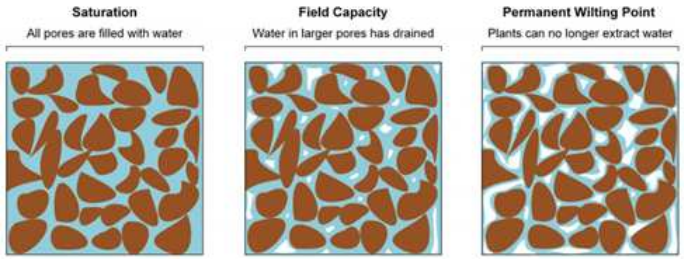

Figure 5.8: Soil water content at saturation, field capacity and permanent wilting point thresholds (Datta et al., 2017)

These potential points are important because from them the Available Water Capacity (AWC) is usually calculated, defined as the difference between the water present at field capacity and that present at the wilting point, i.e., the amount of water that can be used by the plant.

The three potential points were calculated for the specific samplings thanks to the modeling system for estimating soil water balance and crop development CRITERIA (CRITERIA - Modello Di Bilancio Idrico E Sviluppo Colturale, n.d.), made available by Arpae's Climate Observatory and used for estimating seasonal irrigation forecasts in Emilia-Romagna. This model includes two main software (CRITERIA-1D/GEO and CRITERIA-3D), to respectively simulate the water balance of crops considering soil water fluxes and to simulate the water balance of small basins in a three-dimensional domain considering surface and subsurface water fluxes.

To determine the potential points of interest, the first of the two software packages was used, which contains a tool, "SOIL-EDITOR". This tool allows modifying soil properties to estimate water retention and hydraulic conductivity curves based on the Van Genuchten-Mualem model, to date one of the most widely used for calculating these values, but it also provides estimates of potential water balance points based on the different soil parameters entered (percentages of clay, silt and sand, bulk density, etc.), of interest for this thesis work.

These values are summarized in Tab 5.3 of section 5.2.4.

Saturated hydraulic content

The saturated hydraulic conductivity (Ksat) of soil is a measure of the ability of a saturated soil to transmit water when subjected to a hydraulic gradient (Staffilani, 2017), a condition that occurs during very heavy rainfall, under particular morphological conditions or in the presence of surface water tables. This characteristic depends both on the geometry of the pores and the fluid saturating them, and on the texture and presence of organic matter.

For the samplings considered, the saturated hydraulic conductivity value can always be downloaded from the Emilia-Romagna Region's 3D Geoportal (Geoportale 3D, n.d.). The soil of the Copparo area considered is divided into different classes of Ksat, as can be seen from Fig. 5.9.

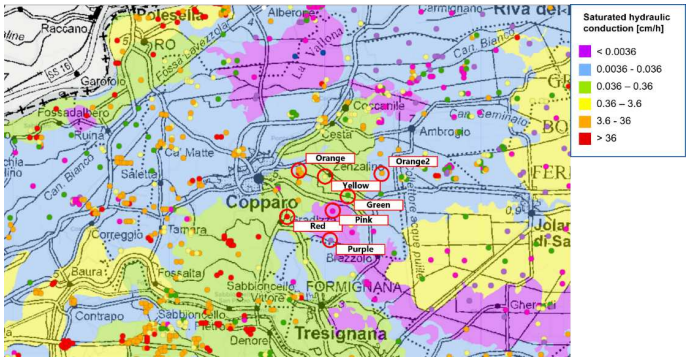

Figure 5.9: Saturated hydraulic conduction of the Copparo area (Geoportale 3D, n.d.)

The map, whose values date from the 2018 sampling year, depicts the areal distribution of soil Ksat classes according to the scheme of the Soil Survey Manual, 1993 [Tab. 5.1] in the polygons of the 1:50,000 scale Plain Soil Map.

Table 5.1: Ksat classes [cm/h] in Emilia-Romagna (SSM, 1993)

KSat	Class	cm/h
1	Very low	<0.0036
2	Low	0.0036-0.036
3	Moderately low	0.036-0.36
4	Moderately high	0.36-3.6
5	High	3.6-36
6	Very high	>36

For each polygon, the weighted average value of Ksat was calculated based on the percentage of soil spread in it. Tended to be clay and silty soils have low saturated hydraulic conductivity and constitute about 44% of the lowland area, while sandy or sandy silty soils have high saturated hydraulic conductivity, although they constitute about 4% of the lowland area (Staffilani, 2017).

As can be seen from Fig. 5.9, the samples selected for the simulations in this thesis work belong to different ranges of hydraulic conductivity, and for each of them the intermediate value of the indicated range was selected because the precise value was not reported in the 3D Geoportal.

Runoff curve number

The runoff Curve Number (CN) is a parameter used to identify runoff or infiltration of water into the soil following heavy rainfall (Woodward et al., 2003). The method of identifying runoff CN was developed by the USDA Natural Resources Conservation Service, and thus depends on both precipitation and infiltration or amount intercepted by crops, according to the formula:

$$\begin{cases} 0 & \text{for } P \leq I_a \\ \frac{(P-I_a)^2}{P-I_a+S} & \text{for } P > I_a \end{cases} \tag{5.1}$$

where Q is the runoff [l], P is rainfall [l], S is the potential maximum soil moisture retention after runoff begins [l] and I_a is the initial abstraction [l].

This value also depends on various soil factors and is therefore based on the assumption that soils within the same climatic region are similar in depth, infiltration capacity, texture, structure, and water table depth, and therefore have the same runoff response, i.e., surface runoff (United States Department of Agriculture, 2022).

For this reason, soils are divided into different groups (A, B, C, D) on the basis of their runoff potential, where group A consists of all soils with high infiltration rates (generally sandy soils) and low runoff potentials, while group D has low infiltration rates (generally clay soils) and thus high runoff potentials. In the case of coexistence of two prevalent groups, soils are indicated by both letters, e.g. A-D.

Runoff potentials have been empirically calculated for different categories of soils, from urban to agricultural to arid and semi-arid (United States Department of Agriculture, 2022). The USDA's "Runoff Curve Number Method" thus involves cross-referencing information such as hydrologic group, land use, cropping practices, and hydrologic condition of soils.

To determine the runoff value for the samplings considered, reference was first made to the dataset that the Emilia-Romagna Region makes available called *Mappe Applicative - Carta dei Gruppi Idrologici della Pianura Emiliano-Romagnola* (Staffilani, 2015). The dataset describes the areal distribution of soil Hydrological Groups through polygons at a scale of 1:50,000, as in Fig. 5.10.

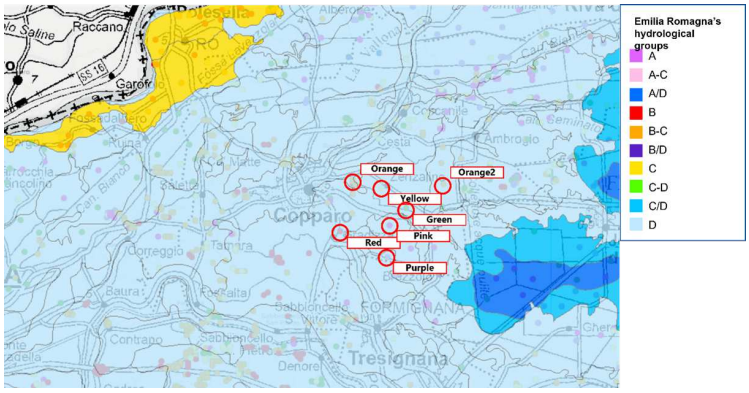

Figure 5.10: Map of hydrological groups of the Emilia-Romagna plain (Geoportal 3D, n.d.)

From the map [Fig. 5.10], it is clearly observed that the prevailing hydrological group of the sampled soil is D (specifically, in the selected sampling area it is D = 96% and B = 4%). To

estimate the runoff potential, as required by the DSSAT, the calculation of runoff Curve Number was then carried out, identifying the type of cover description most suitable for potato cultivation. In particular, to define the most suitable cover description for potato cultivation, the classification made by Kincl et al. (2021) was taken as a reference. Kincl estimated that for a soil with Average Runoff Conditions (ARC-II), the number of runoff curves for potato cultivation was 78 for hydrological group B, thus corresponding to the "Raw crops - straight row" cover group (United States Department of Agriculture, 2022).

The runoff Curve Number corresponding to the same cover group was then chosen, but for hydrological group D, i.e. 89.

Runoff rate

Runoff (or infiltration) rate is the rate at which water penetrates the soil, usually measured by considering the depth of the layer of water that penetrates the soil in one hour. Like the other parameters, infiltration rate depends on soil texture and structure (Food and Agriculture Organization of the United Nations, n.d.).

This value is very complex to calculate, however, the Food and Agriculture Organization (FAO) provides a table [Tab. 5.2] with basic infiltration rates for various soil types, which were used as a reference in the various simulations.

Table 5.2: Basic infiltration rates for various soil types (Food and Agriculture Organization of the United Nations, n.d.)

Soil type	Basic infiltration rate (mm/h)
Sand	less than 30
Sandy loam	20-30
Loam	10-20
Clay loam	5-10
Clay	1-5

Albedo

The last soil value required by DSSAT is albedo, which is the fraction of incident solar radiation that is reflected in all directions based on the surface on which the radiation impacts. The albedo value can range from 0 to 1, from 0.9 for snow to very low values for dark soils. For the soils considered, reference was made to the typical albedo value of free soil, corresponding to 0.17 (Markvart & Castañer, 2003).

5.2.4 Summary

To summarize, seven different samplings were selected corresponding to different percentages of clay in the soil [Tab. 5.3], and for each of them the values of lower boundary, drained upper boundary, saturated water content, saturated hydraulic content, runoff curve number and albedo [Tab. 5.4] were identified, as well as the identification of the corresponding texture.

As shown in Tab. 5.3, as well as Fig. 5.6, these samples are from soils with four different textures, which differ in the other values listed above. To make the simulations representative, therefore, the number of simulations performed was chosen based on texture as the main component of soil behavior to different factors, and was therefore reduced to four of the seven samplings considered. In the case of the same texture, the sampling with similar clay content was selected from the largest number of samplings in the area.

Table 5.3: Soil samples summary

Color	Sand (%)	Silt (%)	Clay (%)	Texture	pH	OrgMat (%)	K2O [mg/kg]	P2O5 [mg/kg]	Ntot [%]
Orange	22	54	24	S. loam	8.10	1.50	180	22.0	1.50
Or.2	42	38	20	Loam	7.75	0.97	178	58.4	0.40
Yellow	12	55	33	S.c.loam	8.07	2.50	433	74.6	1.33
Red	19	67	14	S. loam	8.14	1.90	142	16.4	0.89
Pink	7	49	44	S. clay	7.97	3.64	311	49.3	1.74
Green	9	54	37	S.c. loam	8.05	1.89	35	35.2	1.00
Purple	8	45	47	S. clay	7.62	3.39	342	41.6	2.05

Table 5.4: Soil water content samples summary

Color	Lower limit $[m^3m^{-3}]$	Drained upper limit $[m^3m^{-3}]$	Sat. water content $[m^3m^{-3}]$	Sat. hydr. content [cm/d]	Runoff CN	Albedo
Orange	0.116	0.364	0.443	1.252	89	0.17
Or.2	0.135	0.372	0.430	1.252	89	0.17
Yellow	0.170	0.379	0.460	4.752	89	0.17
Red	0.116	0.364	0.443	4.752	89	0.17
Pink	0.226	0.392	0.480	0.864	89	0.17
Green	0.170	0.379	0.460	4.752	89	0.17
Purple	0.226	0.392	0.480	0.864	89	0.17

5.3 Parameters: crop management data

Regarding the input data to be entered to simulate potato crop management, DSSAT requires the input of data related to different growth stages, such as: cultivar, planting, irrigation, fertilizer, tillage, chemical applications.

This section will therefore analyse the values used as management input data, which were then held constant for the simulations carried out, for which in fact only the environmental data of radiation intensity, temperature and precipitation were modified.

5.3.1 Cultivar

In this section the DSSAT requires to enter the potato species to be simulated, such as Majestic, Achirana, Atlantic, Desiree and others.

As seen in section 4.2.2, DSSAT uses different indices to simulate inhibition to sun exposure and temperature, inhibition which varies according to the species considered.

For the purposes of the simulations in this thesis work, the "Majestic" species was selected, as it is the most common variety in the area of Ferrara considered and has the most standard agronomic characteristics for cultivation, so as to reduce any uncertainty in the output due to the species considered.

5.3.2 Rotation and planting

In this section, DSSAT gives the possibility to enter the sowing and emergence dates of the crop, i.e. the phase after germination when the plant's defence capabilities are limited, as well as a possible rotation of different crops with others on the considered plot.

With regard to the rotation, potato cultivation on a plot must take into account EU Reg. 1305/2013 (EU Parlament and Council, 2013), which divides crops into main, secondary and miscellaneous on the basis of the length of time they occupy the land. Main crops are defined in this way as they occupy the land for the longest time of the year even with repeated cycles, secondary crops have a cycle of less than 120 days, while miscellaneous crops do not belong to the same botanical genus. Based on this distinction, farms must adopt a minimum five-year crop succession, in which three different main crops must be rotated, both in the introduction and maintenance years. In the specific case of the potato, its return to the same plot after 2 years of a species not belonging to the solanaceous family is permitted. However, in the case of the simulations carried out in this thesis work, as specified in section 5.1, only one reference year was considered, given by the climatology of the last six years (2017-2023), and therefore only the presence of the potato crop on the plot was analysed.

As far as the sowing period is concerned, this varies significantly depending on the species, climatic conditions, soil and cultivation techniques of the area considered (Giovannelli et al., 2006). For Emilia-Romagna, the indications present in the Technical Norms were taken as reference (Disciplinari Di Produzione Integrata – Norme Tecniche per Le Colture Orticole – Patata, 2022).

The potato has no restrictions as regards sowing, which is carried out approximately two weeks after the last thaw, identified for the Ferrara area as corresponding to April 15^{th}. Consequently, the emergence period takes place approximately one week later, i.e. around April 23^{rd} (Pavlista, 1995).

The other parameters required for the planting phase were also taken from the Emilia-Romagna Technical Norms, which set the dry seed as as the sowing method for potatoes, distributed in rows, with a population density of 5-7 $plants \cdot m^{-2}$ and a row spacing of 75-90 cm and a planting depth of 10-12 cm. As for the orientation of the cultivation, it was set at 0° from the North to follow the orientation of the rows of an agrivoltaic field, positioned in this way to maximise electricity production thanks to the trackers.

5.3.3 Irrigation

With regard to irrigation, DSSAT allows it to be defined in two ways: by indicating the date of irrigation, the quantity and the mode (e.g. drip or trickle, flood, furrow, etc.) or automatically when required by the soil.

For the simulations carried out in this thesis work, the second mode was preferred as it is more

dependent on daily weather conditions. In fact, the threshold of the maximum available percentage, below which irrigation would have to be carried out, and the end point, above which irrigation would have to be stopped, were indicated.

As far as the threshold is concerned, according to the FAO (Food and Agriculture Organization of the United Nations, n.d.) since the potato is relatively sensitive to soil water deficits, total water should not be reduced by more than 30-50%, otherwise the risk of lower yields is particularly significant, especially in the tuber's early and yield-forming periods, while the early vegetative states and the ripening period are less sensitive. Regarding the end point, again the FAO indicates that the moisture content must be kept relatively high, without, however, causing problems with soil aeration due to the moist and heavy soil, nor problems with a low temperature, the optimum value of which should in fact be between 15-18°C.

For these reasons, 50% and 70% were chosen as threshold and end points respectively.

Regarding the irrigation method, it was opted for the most widespread method to date, i.e. the "drip or trickle" method, which consists of pipes on the surface of the soil that allow drops to drip at a constant rate and quantity from holes at a given distance (usually between 0.15 and 0.3 m between plants, and 0.75 and 0.9 m between rows) (Irriframe - Il Portale Dell'irrigazione ANBI, n.d.).

Due to the very high precision of irrigation and its adaptability to the development needs of the plant, this technique is often associated with the dispersion of fertilizers in the soil, a technique known as fertirrigation. However, for the purposes of the simulations in this thesis work, it was preferred to divide these two management procedures in order to carry out sensitivity studies avoiding correlations between the two techniques.

5.3.4 Fertilizers

The fertilizer-related module is structured in DSSAT with the request to enter data such as the date of application, the type of fertilizer, the application of the fertilizer, the depth at which it was applied, and the quantity in $kg \cdot ha^{-1}$ of N, P, K of that fertilizer.

To determine the quantity of fertilizer to be applied in the simulations, the Emilia-Romagna Technical Norms were taken as a reference, again indicating the different quantities of N, P and K to be applied to a soil depending on its composition, specifically by means of a worksheet made available on the Region's portal (Disciplinari Di Produzione Integrata - Norme Tecniche per Le Colture Orticole - Patata, 2022).

These specify:

- Vegetative group: such as arboreal, horticultural, herbaceous, forage, etc. In our case, therefore, we are referring to horticultural crops.
- Crop: i.e. the particular species of the vegetative group, in this case therefore the potato.
- Cultivation phase/cycle, in this case spring-summer < 70 days.
- Cultivation method and location: open field in a plain bordering urbanised area.
- Expected and proposed annual yield: an average value of approximately 45 $t \cdot ha^{-1}$ was chosen.
- Soil characteristics: percentages of sand, clay, silt and the other data in Tab. 5.3.

- Agronomic practice: the choice of the precession crop was made considering the indication of the Emilia-Romagna Region, in which a crop not belonging to the solanaceae family is suggested.

Based on these values, the recommended quantities are N = 145 $kg \cdot ha^{-1}$, P = 69 $kg \cdot ha^{-1}$ and K = 300 $kg \cdot ha^{-1}$, which were administered to the soil by means of ammonium nitrate 26-0-0, urea 46%, NP 18/46 and granular Sulphate-potassium-magnesium 30+10 at two different times during the cultivation period of the crop: before sowing and one week after the emergence period.

5.3.5 Tillage

Tillage for potato cultivation is only restricted in the Emilia-Romagna Technical Norms for land with an average slope, understood as the percentage ratio between the change in altitude and the distance between the two vertices of the plot, greater than 30%, or for slopes between 10 and 30%, for which limitations are indicated on the type of seeding (e.g. sowing on hard standing for herbaceous crops) and the depth of cultivation.

In the case of the simulations carried out in this thesis work, however, flat land was taken into consideration, since the average slope of the area is almost zero. In fact, considering the map of "Elevated Points - 1:10,000 (Digital)" (Geoportale 3D, n.d.) of the area considered in Copparo [Fig. 5.11], these surveys always have altitudes of 1-2 m a.s.l., thus suggesting that the average slope of the area is not significant. In fact, the contour lines of the area are not available on the portal, which would have allowed a more accurate measurement of the slope of the areas considered.

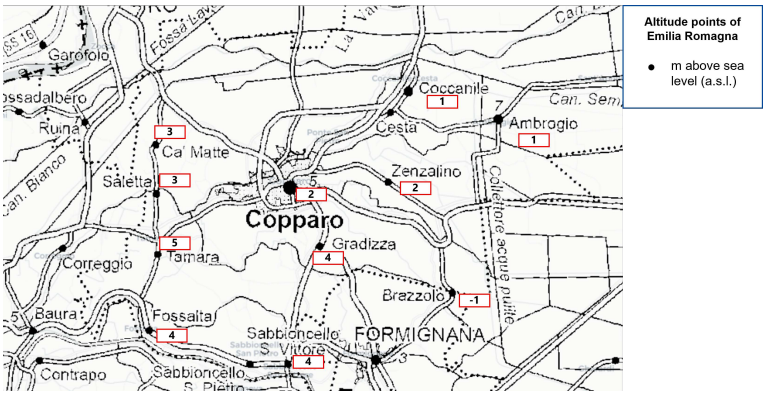

Figure 5.11: - Listed points 1:10,000 (in black) - Copparo (FE)

For this reason, as there are no particular constraints given by the Emilia-Romagna Region, standard soil tillage was studied, which is divided into different categories based on the time of execution and the purposes with which they are carried out (Djaman et al., 2022). These include:

- Cultivation tillage: these are all those tillages used to prepare the land for cultivation, when it has never been cultivated before or is to host a crop for a long period. Of these, the most important are boning and breaking up.
- Main preparatory works: these are carried out before sowing and serve to prepare the soil for sowing; they include ploughing, spading, milling and scarifying.
- Complementary works: these also serve to prepare the soil for sowing, but through actions to improve the plot. These include: grubbing, levelling the surface, harrowing, milling,

rolling.

- Consecutive tillage: these are those that are carried out when the crop is already present on the land, in order to achieve the set objectives. These are therefore specific to the crop present, and include harrowing, scarifying, weeding, rolling and milling. In the case of potato cultivation, only tamping is mainly carried out.

For potato cultivation, the soil does not have to undergo any special tillage, so only tamping is required approximately one month after sowing, so in the case of the simulations around mid-May, to a depth of approximately 10 cm (Djaman et al., 2022).

5.3.6 Chemical applications

DSSAT provides different types of chemicals that can be used for pest and weed control.

Integrated pest management was regulated by EC Directive No 128 of 21 October 2009, which defined pest management as "all available methods of plant protection [...] aimed at discouraging the development of populations of harmful organisms while respecting the environment and human health" (Arsac, 2021). Integrated pest management therefore differs from more traditional chemical pest management, which aimed solely at damage elimination, because it aims to achieve a cost-effective balance that respects the environment and health.

Weed control, on the other hand, or weed control, is the practice of eliminating or containing weeds in order to reduce the damage they cause to crops. Weeding can be done either by chemical herbicides, agronomic measures or biological means.

For potato cultivation, the indications make it clear that chemical soil sterilisation is not allowed (Disciplinari Di Produzione Integrata - Norme Tecniche per Le Colture Orticole - Patata, 2022), while for weed control and defence, only active ingredients are allowed under the limitations of use laid down. In general, the maximum volumes of plant protection products in full vegetation must not exceed a total of 1,000 $l \cdot ha^{-1}$.

However, as DSSAT has been programmed by an international community, the list of possible chemicals that can be used for these purposes consists of several products whose use is not permitted in Italy to date. For this reason, it was decided not to use chemicals for this purpose, postponing to later analysis the influence of these on the final yield in cases of crops with shading.

5.3.7 Harvest

In contrast to irrigation, the date of crop maturity cannot be automatically determined by DSSAT for the SUBSTOR-potato model by the indication to harvest "at maturity", as is possible for other crop models.

For this reason, the ripeness of the Majestic potato crop, which is a semi-delayed ripening species, was defined manually, at just over 130 days from sowing day. Therefore, 31 August was indicated as the time of harvest maturity when the green canopy covers 20% of the ground. This was set considering the harvest of small, medium and large potatoes.

5.3.8 Environmental modifications and treatments

Finally, the simulations with DSSAT to model the effect of shading on potatoes were performed using the "Environmental modifications" module, in which the software allows the modification of daily environmental conditions such as daylength [h], radiation $[MJ \cdot m^{-2} day^{-1}]$, maximum daily temperature (°C), minimum daily temperature (°C), precipitation (mm), CO_2 (vpm), dewpoint temperature (°C) and wind $[km \cdot day^{-1}]$

Each variable can be modified either from specific dates or from the start of the simulation in four different ways: "add", "multiply", "replace" or "substract", with a factor that can be entered at the simulator's discretion. As can be understood, this allows one to add, multiply, replace or subtract a specific value from a specified date to the daily meteorological data entered as input into the simulation.

In the specifics of this thesis work, the radiation, temperature and precipitation variables were modified to simulate the effect of shading and a possible change in temperature and ground water content due to the presence of the photovoltaic modules.

For most of the simulations, the percentage of radiation loss was not associated with a particular agrivoltaic configuration, but was progressively decreased by 10% to first understand the dependence of the crop on radiation.

Once all the above data had been entered and the appropriate environmental modifications had been made, the software allowed different levels of Treatments to be simulated. These levels were characterised by having the data of cultivar, soil analysis, planting, fertilisers, chemical applications, tillage constant, and by varying only the environmental modifications, resulting in 11 distinct levels: the first level simulating a scenario without panels, and therefore without any environmental modification, and the next 10 levels in which the radiation impacting the crop is progressively reduced by 10%.

Chapter 6

Results and discussion

In this chapter, simulations of the effect of different shading scenarios on the potato crop are presented and analyzed, challenging the SUBSTOR-potato model to understand its sensitivity and determine the main parameters affecting crop growth. For this reason, the analysis is divided into four different phases:

1. *Evaluation of initial conditions*: in this phase, it was verified that the simulations obtained were consistent with the harvest data actually recorded in the Ferrara area, considering the climatology of the six meteorological years under analysis.
2. *Study of annual harvest variability*: the annual variation in harvest as a function of different meteorological conditions was verified to also validate the hypothesis of using climatology as the reference meteorological year.
3. *Statistical and sensitivity analysis*: at this stage, the variations in the harvest obtained over the six years were analyzed to relate them to the annual variations in different parameters, such as radiation, temperature and precipitation, in order to identify which of these had the greatest impact on the final harvest and on the shading response.
4. *First estimation of the harvest in three different possible agrivoltaic configurations*: harvest yields in the agrivoltaic configurations with 2P trackers of standard height and pitch at 10 and 14 m, and that with panels at 4 m height and pitch at 5 m were studied in particular.

Before proceeding with the steps listed above, the software was also put to the test to verify its reliability by inserting some initial growing conditions for the vegetable that were not suitable for its growth (e.g., planting in early January, Fig. 8.1 in the Appendix), obtaining from the model a consistent response, i.e., of zero harvest.

6.1 Initial conditions assessment

In order to proceed to the assessment of the initial conditions to be considered as optimal on which to subsequently carry out the reasoning on the best agrivoltaic configuration to be adopted, all the data set out in Chapter 5 regarding soil, planting, irrigation, fertilizers, chemicals, tillage and harvesting were entered.

As for the data related to crop management, these have little intrinsic variability, as they are either regionally standardised or automatically defined by the software during the various crop growth phases.

The factors of greatest variability are therefore related to the different chemical-physical and hydrological characteristics of the samplings considered, which is why the choice of the reference soil was made by varying only these parameters.

As reported in Tab. 5.3 in section 5.2.4, there are four different soil textures in the Ferrara area to be considered: silt loam, silty clay loam, silty clay and loam.

For each of these, a simulation was carried out of how the harvest varies as a function of radiation loss [Fig. 6.2], progressively decreasing the daily radiation percentage by 10%, to observe the harvested yield predicted by the model in soils with different textures. As mentioned before, in the case of different samplings of the same texture, the data of pH, organic matter, K_2Oass, P_2O_5ass, N_{tot} entered were those of the largest number of similar samplings in the area considered on the basis of clay content. Therefore, for the silt loam, the orange sample was taken as reference, for the silty clay loam, the yellow sample was considered, and for the silty clay, the pink sample was considered.

With regard to the meteorological data considered in these simulations, the climatology of the last six years was used, in order to eliminate climatic variability and only study the effect of the different soils.

Finally, before proceeding with the analysis of the results, it should be noted that the software returns a harvested yield measured in kg[dm]/ha, i.e. the amount of dry matter of potatoes harvested per hectare. It tends to be the case that most potato varieties have a water content of between 75-80%, and thus have a dry matter of around 20% (Kapoor et al., 2019), as can also be observed in Fig. 6.1.

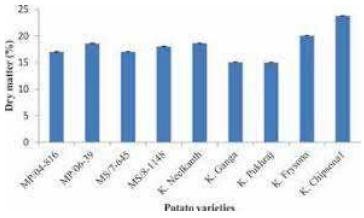

Figure 6.1: Dry matter content [%] of different potato varieties (Kapoor et al., 2019)

Below are the results obtained for the four different soil textures:

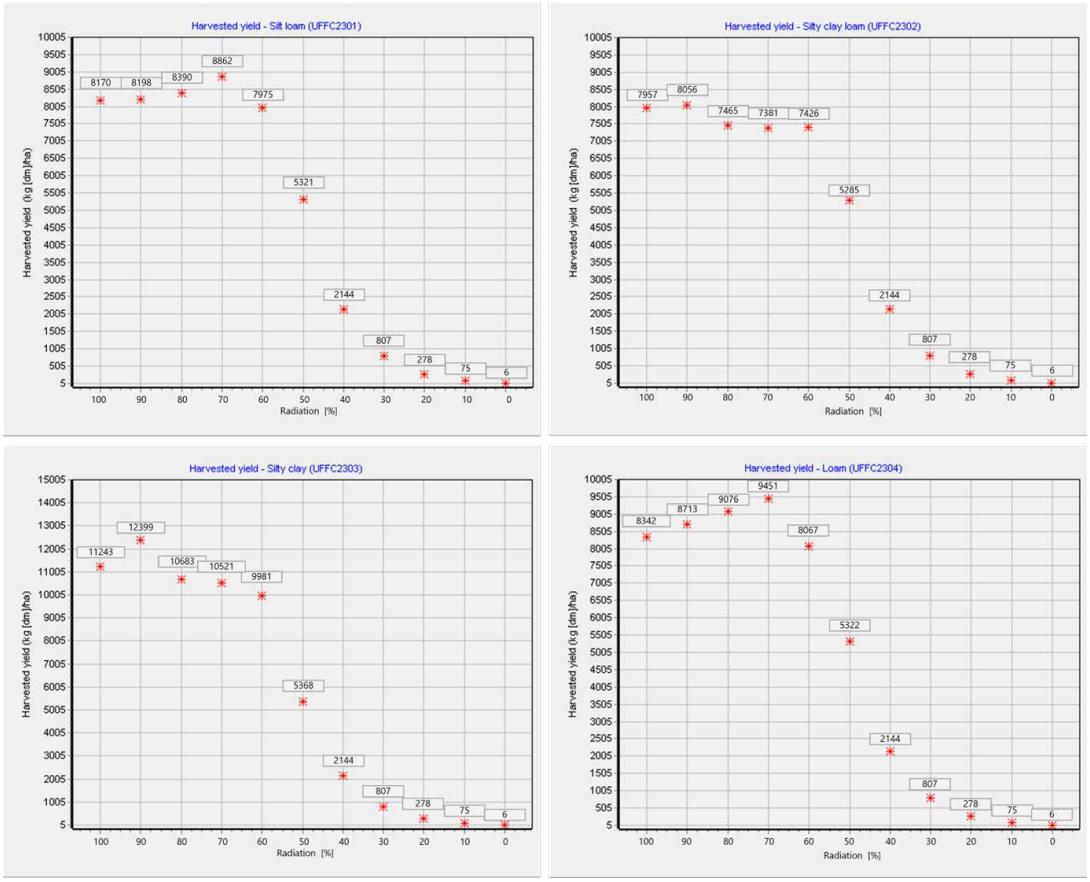

Figure 6.2: Shading simulations for different texture sampling

As can be seen from Fig. 6.2, all the simulations on the different soil types show similar behaviour, i.e. they maintain an almost constant (if not increasing) harvest up to about 60% of incident radiation, i.e. up to the 40% shading scenario.

To verify the reliability of the output of these simulations, the expected harvest in the scenario without panels, i.e. with 100% incident radiation, was compared with the average annual potato harvest in the Ferrara area corresponding to about 40-55 $t \cdot ha^{-1}$ (Disciplinari Di Produzione Integrata - Norme Tecniche per Le Colture Orticole - Patata, 2022). Since the dry content of the potato is about 20% of the total weight, the expected yield from the various simulations, on average 8,928 $kg[dm] \cdot ha^{-1}$ and corresponding to 44.6 $t \cdot ha^{-1}$, is in line with the average recorded in the Ferrara area.

The choice of soil on which to carry out the subsequent simulations therefore fell on two factors: the type of texture most commonly used to cultivate potatoes and that most widespread in the area.

According to the literature, in fact, the optimal soils are of different types: some indicate loamy sand and sandy loam soils as the optimal ones for potato growth, thanks to their good response under full irrigation (Ahmadi et al., 2010), while other studies indicate loam soils as the most suitable and with an incremental production response (Miller & Martin, 1983). In fact, this response was also observed in the simulations of Fig. 6.2; however, silt loam soil was chosen as the reference terrain in order to observe the harvest prediction even in soils that are not fully optimal

for cultivation but that have a percentage of silt that is widespread in the Copparo area. The simulations performed can obviously also be carried out on optimal textures, such as loam and sandy loam, in subsequent in-depth studies.

As can be seen always from Fig. 6.2 for the scenario of cultivation on silt loam soil, therefore, the potato crop remains constant up to about 60% of incident radiation, with an 8% increase in production in the scenario with shading at 30%. At 50% incident radiation, however, the yield predicted by the simulation reaches 5,321 $kg[dm] \cdot ha^{-1}$, thus registering a decrease of 34.8%.

6.2 Annual crop variability

The result of the previous paragraph was obtained by taking the six-year climatology (2017-2022) as a meteorological reference. However, both to assess the overall reliability of the climatology as a reference year and to understand the main parameters that affect the final crop yield, it is necessary to study the variation of the harvest for the different shading scenarios considering the weather variability of the individual years.

For this reason, the final crop yield was simulated by keeping all crop management and soil composition parameters unchanged, always taking the silt loam textured soil as a reference, and only the input meteorological conditions corresponding to the different years were varied (Dataset Meteo Orario E Giornaliero Dal 2001 - Dati Arpae, n.d.).

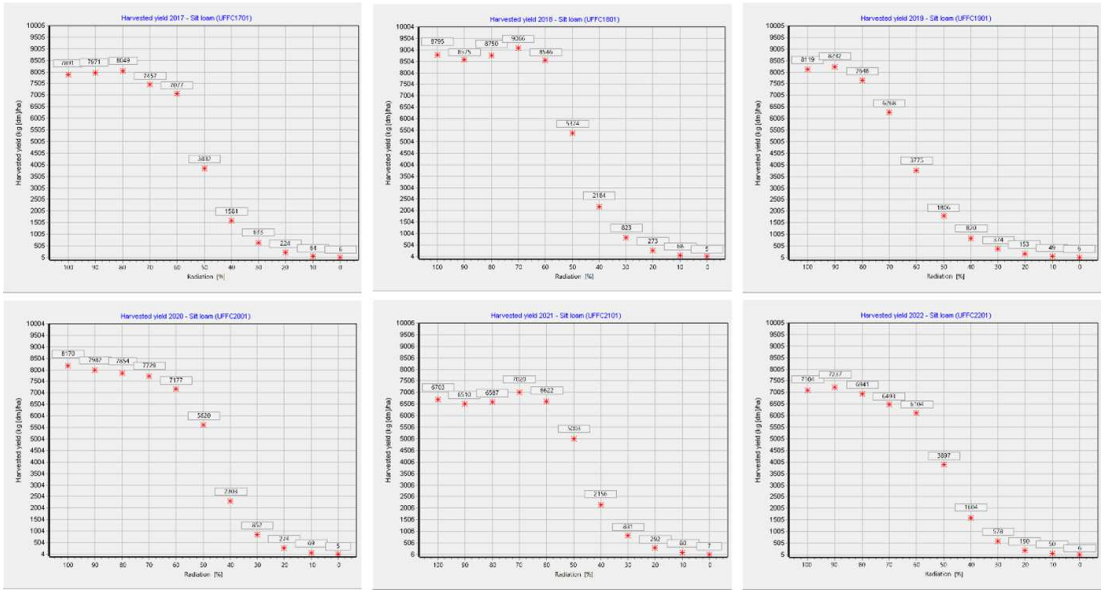

Figure 6.3: Harvested yield under different shading scenarios (2017-2022)

As can be seen from Fig. 6.3, the decreasing trend as shading increases, initially linear and exponential from a percentage of incident radiation, is similar for all years considered.

Therefore, in order to affirm that the climatology considered above for the simulations in section 6.1 is usable as a reference meteorology, a Mann-Whitney test was carried out between the most dissimilar distribution in Fig. 6.3 (from the year 2019) and the one obtained using the climatology

for the same soil texture. The Mann-Whitney test is a non-parametric test that is used instead of the t-test when samples, as in this case, do not follow the normal distribution and are independent. The null hypothesis of such a test is that the tested distribution (of the year 2019) is equal to the distribution obtained through climatology. The result of this test was: the U-value is 47.5. The critical value of U at $p < 0.05$ is 34. Therefore, the result is not significant at $p < 0.05$. The z-score is 0.82081. The p-value is 0.20611. The result is not significant at $p < 0.05$. The two simulations are therefore similar, and the climatology can be used as a reference for subsequent simulations, carried out in section 6.5.

However, in order to understand the actual variations in different years in more detail, it is necessary to consider the differences in harvested yield of the different shading scenarios compared to the scenario without panels, in Tab 6.1.

Table 6.1: Percentage differences in production between different shading levels and the scenario without panels

Year	Δ 10% [%] (90% rad)	Δ 20% [%] (80% rad)	Δ 30% [%] (70% rad)	Δ 40% [%] (60% rad)
2017	1.01	2.00	-5.50	-10.32
2018	-2.52	-0.53	3.06	-2.85
2019	1.39	-5.80	-22.80	-53.50
2020	-2.30	-3.87	-5.40	-12.15
2021	-2.88	-1.73	4.63	-1.21
2022	1.87	-2.29	-8.60	-14.08

As can be seen from Tab. 6.1, the drops in production yield based on the shading percentages considered differ slightly for the different years. In particular, three different responses can be observed, considering 5% as the acceptability limit for considering the production yield comparable:

- *Category 1 - Production drop at approx. 80% incident radiation*: this response to shading is recorded for only one year, 2019, with 5.80% less production than in the scenario without panels. In fact, if we consider the harvest of the same year at 70 and 60% incident radiation, we can see how this drops significantly, reaching 53.50% less yield than the harvest of the same year without panels.
- *Category 2 - Production drop at approx. 70%*: this intermediate scenario is recorded in the rest of the other years, 2017, 2020 and 2022, resulting in production drops of around 12% with the incident radiation scenario at 60%.
- *Category 3 - Production drop at approx. 60%*: this response is recorded for two years, 2018 and 2021, for which there is also an increase in production to 70%, as in the initial simulation of Fig. 6.2 where the reference meteorological year was climatology

These variations can also be summarised by means of the boxplot graph in Fig. 6.4, which clearly shows how the distribution of final yields varies significantly from 60% incident radiation onwards, becoming more pronounced at 50%.

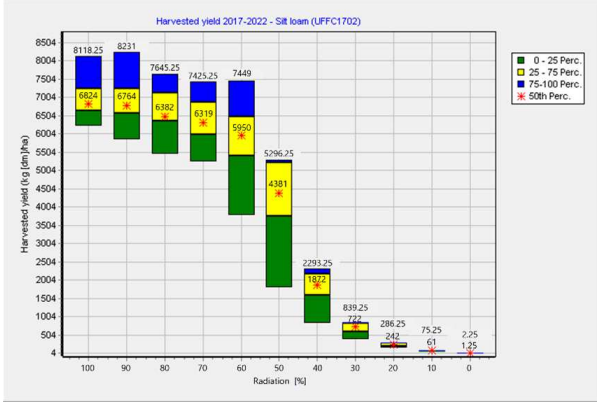

Figure 6.4: Harvested yield 2017-2022

This boxplot obviously takes into account not only the response to shading, but also the absolute crop yield in different years.

In fact, in addition to the effect of shading on the production yield, the simulations in Fig. 6.3 show that the absolute yield (observed in the scenario without panels, with 100% incident radiation) differs quite significantly between the different years. In particular, the following categories can be distinguished with regard to production:

- *Category a - High production (approx. between 8,900 and 9,100 kg[dm]/ha)*: 2018 has a good response to shading (60% drop in incident radiation) and a higher absolute production than the average of the years.
- *Category b - Average production (approx. between 7,900 and 8,100 kg[dm]/ha)*: for the years 2017, 2019 and 2020. Therefore, despite the fact that 2019 has a significant drop in production with shading, the average crop yield remains rather high until the exponential decrease begins.
- *Category c - Low production (approx. between 6,800-7,100 kg[dm]/ha)*: 2021 and 2022 have a not particularly strong response to shading (60-70%), but a lower absolute production than the other years.

For this reason, it was studied which parameters clearly varied between the different meteorological years considered, so as to understand which of them had the greatest impact on the harvest in terms of both shading response and absolute production drop, in order to better size the agrivoltaic field at a later stage.

6.3 Statistical and sensitivity analysis

Among the parameters considered, radiation, temperature and precipitation were analysed for the different years as factors of greatest interest, especially when comparing the year 2019 with the other years, as 2019 was the year in which the effect of shading on the final harvest was recorded as more significant than the others (production drop at 80% incident radiation, i.e. at 20% shading).

In particular, the effect of radiation, which is the one most altered by the presence of the panels, was studied at the monthly level to assess its influence during the different growth phases of the crop. These phases can be seen in Fig. 6.5, where it can be noted that at the end of the first month,

vegetative growth, i.e., the main leaf growth phase of the plant, ends and the tuber initialization phase begins, until bud break, which corresponds to the peak of vegetative growth around day 60.

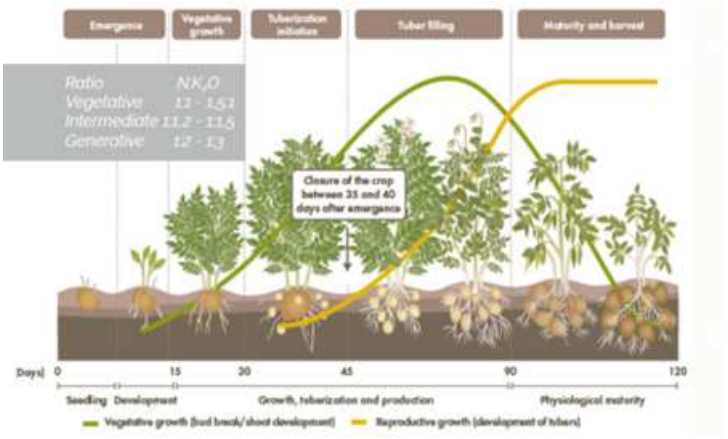

Figure 6.5: Potato growth stages (Potato Vegetative/Generative Growth Balance, 2022)

In the following paragraphs, therefore, it was analyzed how radiation affected in different years the growth of the plant in the first two to three months, corresponding to different vegetative stages, and the relations of this with temperature and rainfall were also studied, as they are closely interconnected in the model.

6.3.1 Radiation

In order to compare the variation of radiation in the first months in the different years considered, taking 2019 as the year of significant variation compared to the others, the integral of the monthly radiation was calculated from mid-January, and mid-April to mid/end of August was then considered as the interval of interest, as the actual cultivation period of the crop in the simulation.

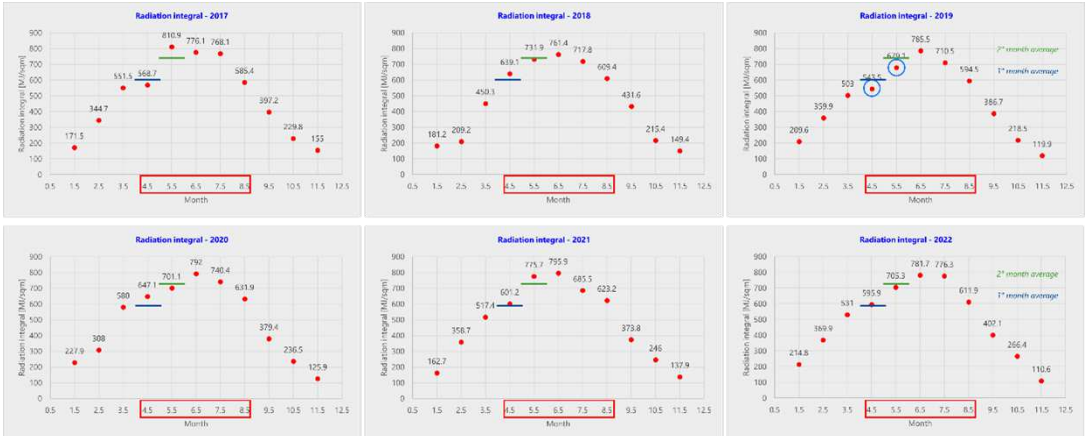

Figure 6.6: Radiation integral for the years 2017-2022. Highlighted the months of interest and the average for the first two months

Fig. 6.6 therefore shows the monthly radiation integral for the different years, with the average cumulative radiation for the first month (599.25 $MJ \cdot sqm^{-1}$) and for the second month (734 $MJ \cdot sqm^{-1}$). Comparing 2019 with the other years, an initial analysis shows that this year saw lower-than-average values of the radiation integral for the first two months of cultivation, while the other months recorded quite similar values.

These differences are evident in the summary graph in Fig. 6.7.

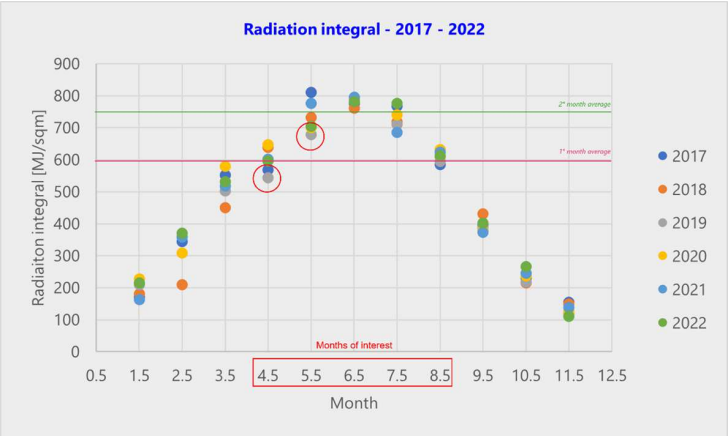

Figure 6.7: Radiation integral - years 2017-2022

Indeed, Fig. 6.7 shows that for the years belonging to the above categories:

- *Category 1 (production drop at approx. 80%)*: in the first two months of interest, the radiation integral for 2019 is lower than the average and the radiation integral for all other years;
- *Category 2 (production drop at approx. 70%)*: 2020 and 2022 have rather similar values of radiation integral in both months, while 2017 has a similar trend to 2021 in both months, but different production drop.
- *Category 3 (drop in production at approx. 60%)*: 2018 shows rather high radiation integrals in the first two months, although slightly below average for the second month; on the contrary, 2021 shows a below-average radiation integral in the first month, while above average in the second month.

These considerations suggest two hypotheses: with regard to the effect of shading, and thus the ideal incident radiation for potatoes, this does not depend solely on the radiation of the individual months, for which no precise pattern can be discerned, but probably on the cumulative radiation of both the first two months; on the other hand, with regard to the absolute annual production, it is possible that this is influenced by other parameters besides radiation.

To test the first hypothesis, the radiation integral was therefore calculated for the first two months, and the test was extended to the third month [Fig. 6.8].

Figure 6.8: 2-3 months cumulative radiation - 2017-2022

As can be seen from Fig. 6.8, the cumulative radiation in the first two months most significantly highlights the differences in shading between the different years considered. In fact, 2019, which has a production drop at 80%, corresponding as can be seen in the graph to 20% shading, records the lowest integral of radiation in the first two months considered together, followed by 2022, 2020 and 2017, which are instead the years with the production drop at around 70% incident radiation. On the other hand, 2021 and 2018 are the years with production drops at 60% and have in fact cumulative radiation in the first two months among the highest.

These differences remain almost unchanged even when considering the three months, although in the long run there are variations that suggest that for the later months other parameters also come into play in defining optimal crop growth.

To further confirm that cumulative radiation is a determining factor for the percentage of shading at which yield loss occurs, harvest simulations were therefore carried out by imposing the different shading scenarios progressively over the different growing months.

Below is just one example for the three different categories: 2019 for category 1 (production loss at 80%), 2017 for category 2 (production loss at 70%) and 2018 category 3 (production loss at 60%); for the other years, see Appendix (Fig. 8.2 - 8.7).

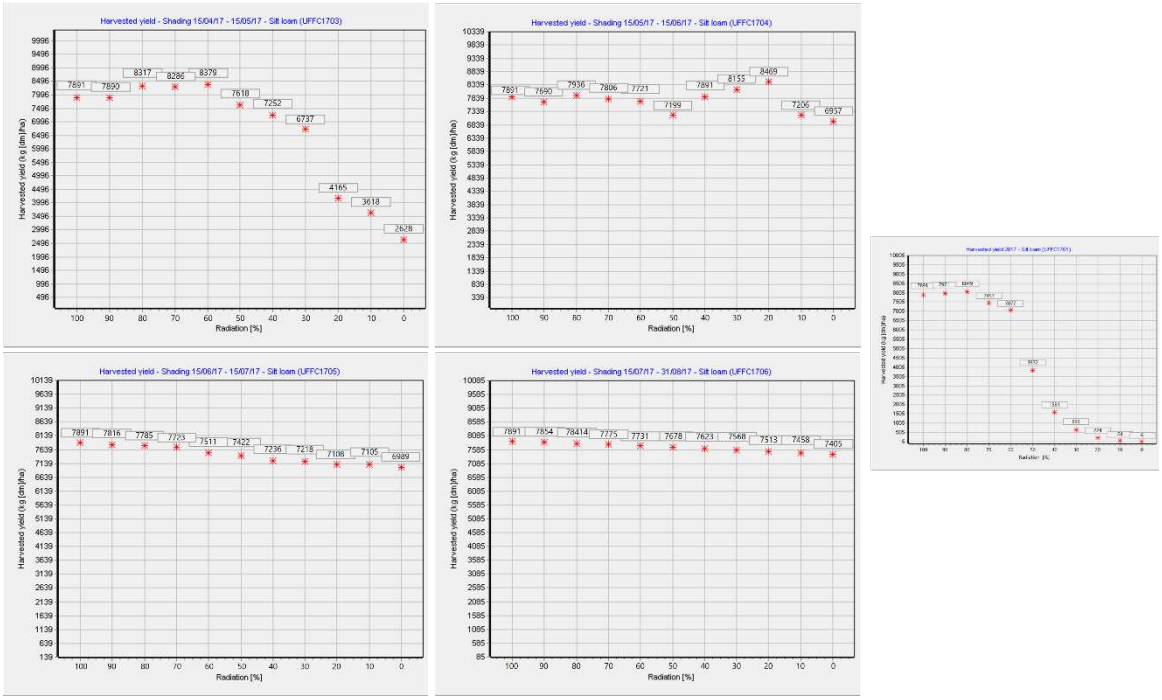

Figure 6.9: Harvested yield under monthly progressive shading scenarios (2017)

In particular, Fig. 6.9 shows the harvested yields by shading only the first, second, third and fourth month of 2017 of potato cultivation, respectively. As can be seen in comparison to the graph on the right in which shading was set for the entire duration of cultivation, by shading the first month the yield loss is significant in the different shading scenarios, although it only decreases by 14% at 30% incident radiation, confirming that it is not only the first month that is decisive for crop growth. The effect of shading becomes less relevant from the third month onwards (with a loss of 11% of the crop at 0% incident radiation), becoming insignificant in the last month of cultivation (6.1% at 0% incident radiation).

However, if, as directly observed from the meteorological data, the cumulative radiation in the first two months and the first three months is considered, the following graphs are obtained [Fig 6.10].

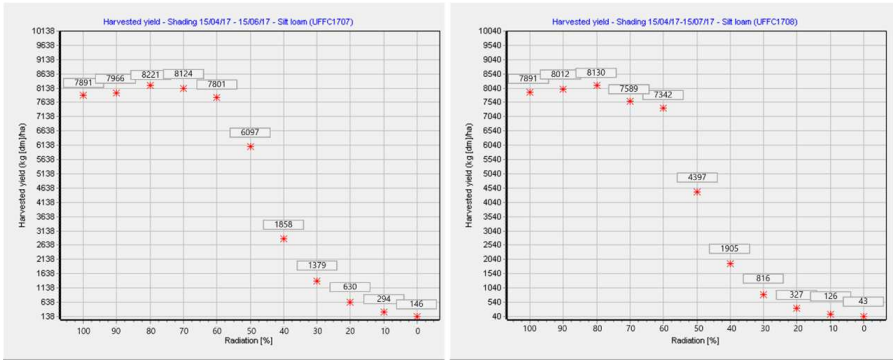

Figure 6.10: Simulations of the crop yield under shading of the first 2 months and the first 3 months (2017)

Fig. 6.10 highlights how these graphs closely resemble the simulation in which shading is imposed for all growing months. To test this hypothesis, the Mann-Whitney test was performed, in which the null hypothesis is that the distribution tested (with shading the first two months and with shading the first three months) is equal to the distribution with shading over the entire period.

Below are the test values obtained by comparing the simulation with shading for all growing months and the simulation with shading for the first few months:

- *One month*: the U value is 34.5. The critical value of U at $p < 0.05$ is 34. Therefore, the result is not significant at $p < 0.05$. The z-score is 1.67446. The p-value is 0.04746. The result is significant at $p < 0.05$. The two simulations differ as expected, so the effect of shading only on the first month is not significant, but the cumulative irradiance on the two and three months should be considered.
- *Two months*: the U-value is 50.5. The critical value of U at $p < 0.05$ is 34. Therefore, the result is not significant at $p < 0.05$. The z-score is 0.62382. The p-value is 0.26763. The result is not significant at $p < 0.05$. This value shows that the two distributions are comparable in that I cannot disprove the null hypothesis, therefore that shading only the first two months results in effects comparable to the shading scenario for all months of potato cultivation.
- *Three months*: the U-value is 55.5. The critical value of U at $p < 0.05$ is 34. Therefore, the result is not significant at $p < 0.05$. The z-score is 0.29549. The p-value is 0.38209. The result is not significant at $p < 0.05$. As expected, the results for the shading simulation for the first three months reinforce the scenario of two months of cumulative radiation.

This verification was also done for the other two categories of simulations (2 and 3). Therefore, the following results are obtained for the year 2019 and 2018 for the different progressive monthly shading scenarios [Fig. 6.11 and Fig. 6.12]:

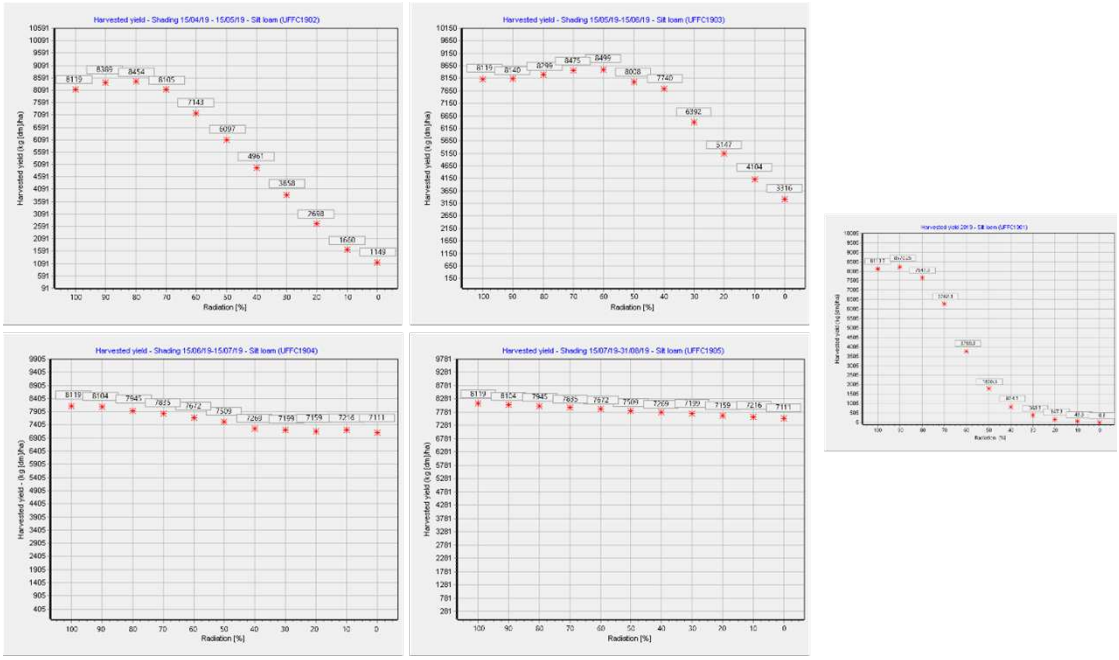

Figure 6.11: Harvested yield under monthly progressive shading scenarios (2019)

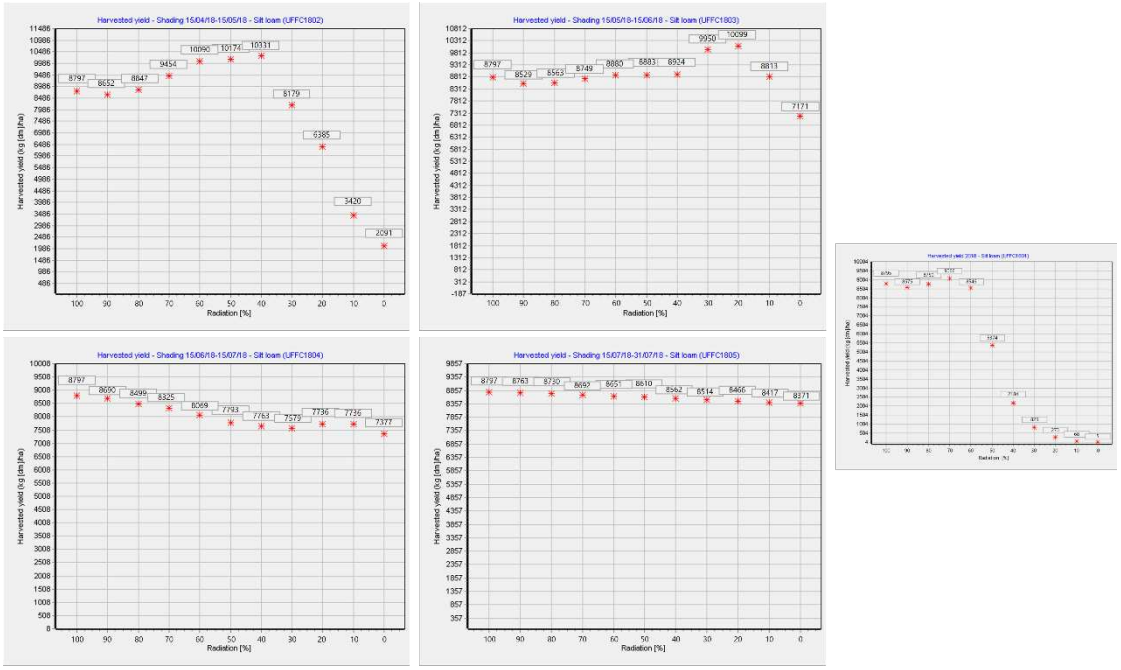

Figure 6.12: Harvested yield under monthly progressive shading scenarios (2018)

As seen for 2017, also for 2018 and 2019 we have that the effect of shading on crop yield loss is found mainly for the first two months, with some residual even for the third month for 2018.

In fact, simulating shading for the first two months and the first three months of the two years considered [Fig 6.13 and Fig. 6.14]:

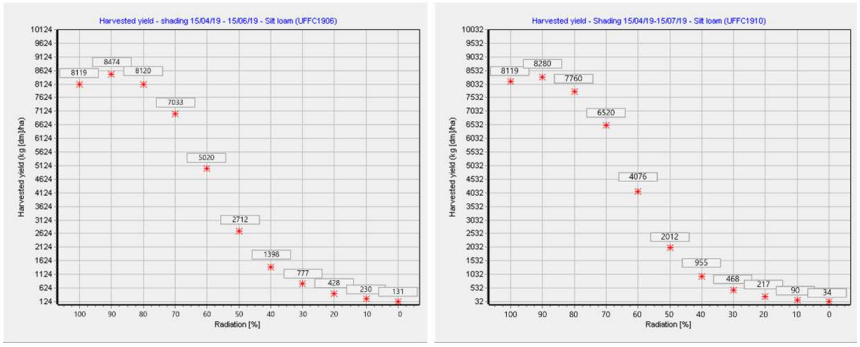

Figure 6.13: Simulations of the crop yield under shading of the first 2 months and the first 3 months (2019)

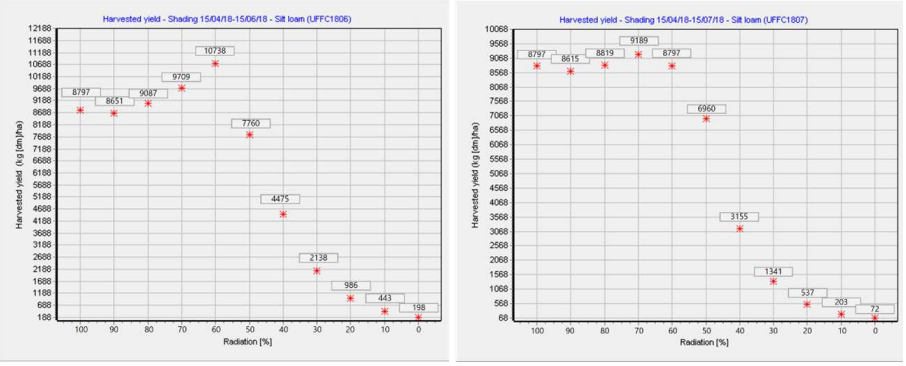

Figure 6.14: Simulations of the crop yield under shading of the first 2 months and the first 3 months (2018)

The following Mann-Whitney test values are obtained by comparing these simulations with that with shading present for all growing months:

- 2019:
  - One month: the U value is 35.5. The critical value of U at $p < 0.05$ is 34. Therefore, the result is not significant at $p < 0.05$. The z score is -1.60879. The p-value is 0.0537. Therefore, the result is not significant at $p < 0.05$. The value is close to the threshold value. The value is close to the threshold value and indicates the near diversity of the two simulations.
  - Two months: The U-value is 51.5. The critical value of U at $p < 0.05$ is 34. Therefore, the result is not significant at $p < 0.05$. The z-score is 0.55815. The p-value is 0.28774. The result is not significant at $p < .05$. The two simulations are comparable.
  - Three months: The U-value is 55.5. The critical value of U at $p < 0.05$ is 34. Therefore, the result is not significant at $p < 0.05$. The z-score is 0.29549. The p-value is 0.38209. The result is not significant at $p < .05$. The two simulations are comparable.
- 2018:
  - One month: the U value is 28. The critical value of U at $p < 0.05$ is 34. Therefore, the result is significant at $p < 0.05$. The z score is -2.10128. The p value is 0.01786. The result is significant at $p < 0.05$. Therefore, even for 2018, shading only the first month, the effect is not comparable to shading for all growing months. Therefore, it is necessary to consider the cumulative radiation for the first two and three months.
  - Two months: The U-value is 46. The critical value of U at $p < 0.05$ is 34. Therefore, the result is not significant at $p < 0.05$.The z-score is 0.91931. The p-value is 0.17879. The result is not significant at $p < 0.05$. The two simulations are comparable.
  - Three months: The U-value is 50. The critical value of U at $p < 0.05$ is 34. Therefore, the result is not significant at $p < 0.05$. The z-score is 0.65665. The p-value is 0.25463. The result is not significant at $p < 0.05$. The two simulaizons are comparable.

These tests thus confirm that the cumulative radiation in the first two months is critical in determining the percentage of shading from which a drop in production loss occurs, as can also be seen from the summary graph in Fig. 6.15.

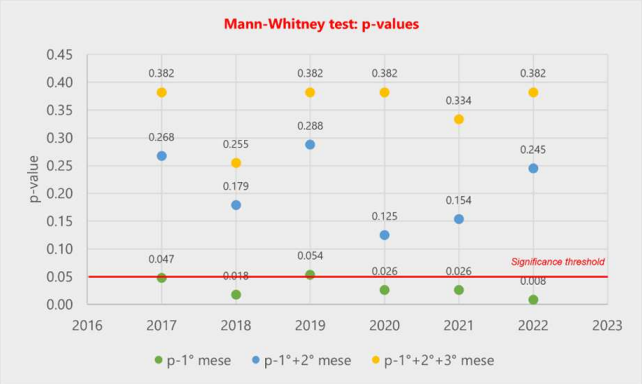

Figure 6.15: p-values of the Mann-Whitney test (2017-2022)

As can be seen from Fig. 6.15, the p-values calculated to compare the distribution with shading on all months and the distributions where shading was imposed only on the first month are all below the significance threshold, thus indicating that the period to be considered to understand the drop in production at a given percentage of irradiance is at least that corresponding to the first two months of cultivation.

Furthermore, this shows that there is an absolute value of incident radiation that must be achieved in the first two months for the crop to remain unaffected until 30-40% shading, which is within the range of (1223,1301) $MJ \cdot sqm^{-1}$, i.e., between the values of cumulative radiation in the first two months of 2019 (year with production decline at 80% radiation) and 2022 (year with production decline at 30% and with lower cumulative radiation than other years with the same production decline), respectively. Therefore, as seen in Fig. 6.8, the production decline in 2019 was due to the low radiation in the first two months, which did not exceed the minimum incident radiation threshold.

This cumulative radiation, on the other hand, does not seem to have correlations with the absolute yield of the crop, in that if the 2019 crop, for example, is considered, it is higher than the 2021 crop, despite the incident radiation being significantly lower for 2019. Therefore, other factors that could affect the total harvest, such as temperature and rainfall, were taken into account.

6.3.2 Temperature

The analysis of the response of crop yield to temperature variation has the dual purpose, on the other hand, of better understanding what factors most influence absolute crop yield, and whether this has any effect on the decrease in yield as shading changes, and then analyzing the effects of a possible rise in air temperature under the panels due to the creation of an underlying microclimate. Note that the temperature parameter varied is only related to air temperature, as it is the only input parameter that can be entered into the software, which automatically calculates the ground temperature from the air temperature and from the boundary conditions of the soil temperature, calculated from the average annual air temperature and the magnitude of the average monthly temperatures. Indeed, the presence of photovoltaic panels is assumed to contribute to a decrease in soil temperature, with potentially positive effects on crop growth. However, the detailed analysis of the different effect of air and soil temperature is deferred to later studies, as it cannot be simulated through the "environmental modifications" section of the software.

As with irradiance, before directly simulating the crop yield for different years by varying the

temperature parameter, the monthly and total weather data for the growing months of the considered years were analyzed. Specifically, the average temperature and the sum of the minimum and maximum temperature, respectively, multiplied by 0.75 and 0.25 were analyzed. This check was done because the software reports the average temperature as the determinant factor for leaf and tuber growth [eq. 4.2, Fig. 4.2] and the weighted sum of the minimum and maximum as the tuber inhibition factor [Fig. 4.3]. For both factors, the model identifies optimal ranges for crop growth, as seen in Chapter 4.

The distribution of the average monthly temperatures recorded for the different years is thus:

Figure 6.16: Average monthly temperature (2017-2022)

According to the model, the average monthly temperature that allows optimal leaf development and vegetative biomass accumulation corresponds to the (17,24)°C range. As can be seen from Fig. 6.16, some years show an average distribution outside this range in the first month (2017, 2019, 2021 and partly 2022), although almost all fall fully within the second month. As with radiation, the average temperature of the first two to three months together was also considered.

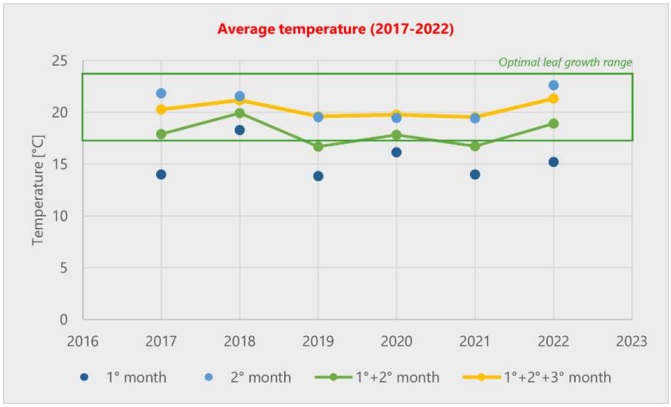

Figure 6.17: Average monthly temperature of the first 2-3 months (2017-2022)

As it can be seen in Fig. 6.17, the years in which, however slightly, the average temperatures fall outside the optimal range for leaf growth in the first two months are 2019 and 2021, which are the

years of highest shading and lowest simulated production, respectively.

Therefore, before verifying whether the temperature factor is a determinant of total production or the percentage of shading at which yield decline occurs, the possibility that this is due to the phenomenon of inhibition of tuber initiation was analyzed, especially to evaluate the years with lower absolute yield. The weighted distribution of minimum and maximum temperatures in different years was then observed, as per Fig. 4.3.

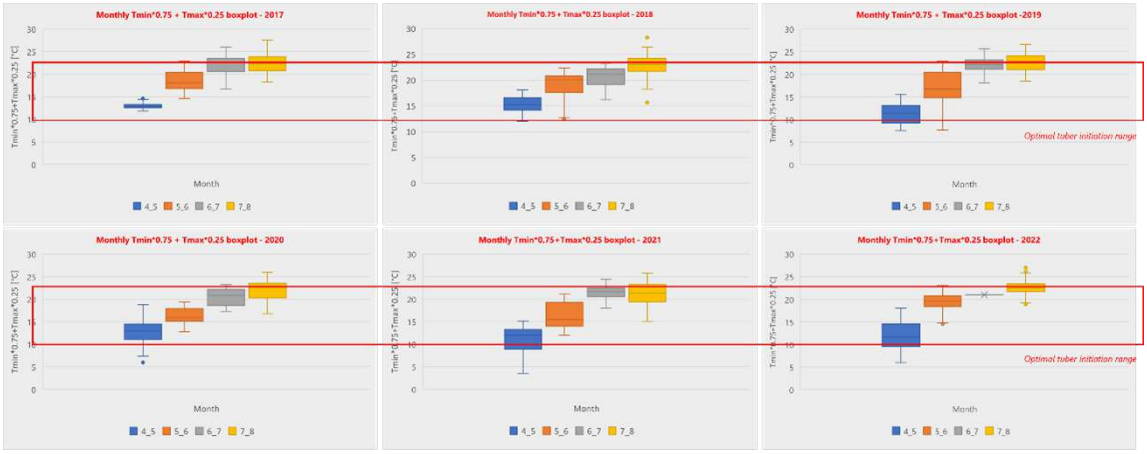

Figure 6.18: Monthly 0.75Tmin + 0.25Tmax (2017-2022)

As can be seen from Fig. 6.18, these temperatures fall within the optimal range (10,23)°C (McGee, 1986) in both the first and second months, so it would not appear that sufficient conditions for tuber growth inhibition occurred in either month. However, further evidence for this was obtained by considering the average temperatures and the weighted minimum and maximum temperatures for the first two and three months [Fig. 6.19], as seen before.

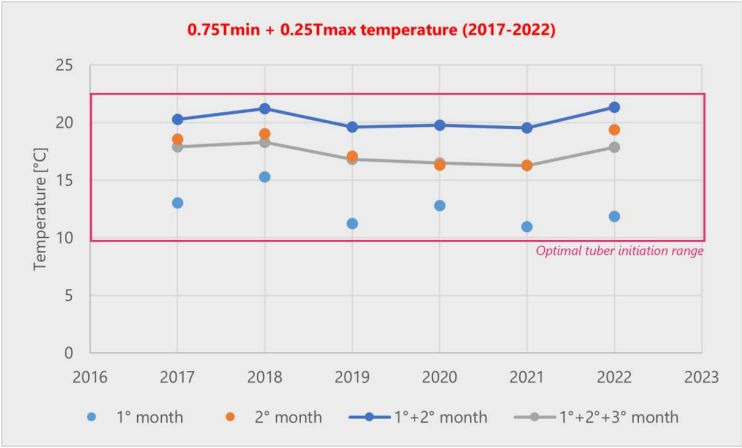

Figure 6.19: Weighted minimum and maximum temperature in the first three months (2017-2022)

The graph in Fig. 6.19 confirms that there was no inhibition in tuber growth, with the average temperature for all the first three months falling within the optimal range.

Therefore, to test the effect of lower average temperatures in the years 2019 and 2021 on shading and absolute production, respectively, 2018 was taken as the reference year for optimal climatic conditions, which in fact has a high absolute production (8,795 $kg \cdot ha^{-1}$) and a very good response to shading (60% production drop).

The year 2021 was then simulated by entering the temperature values of the year 2018, to see if this could have caused an increase in absolute production, thus imputing the low temperatures of the first two months to this amount of harvest [Fig. 6.20].

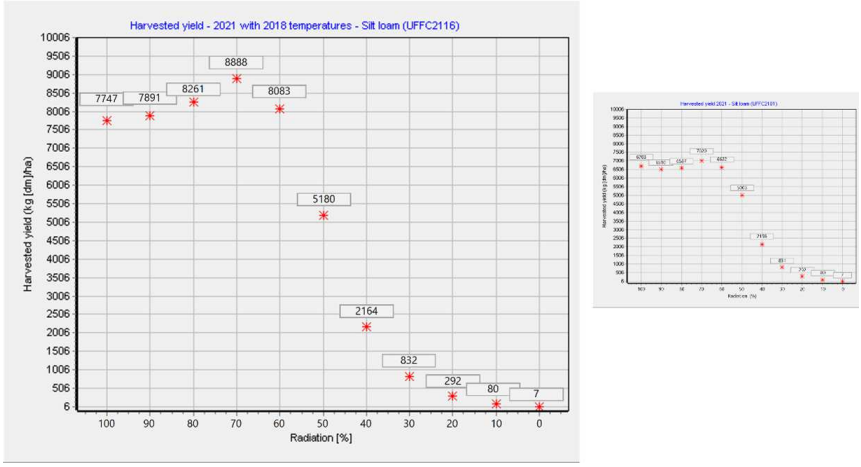

Figure 6.20: Simulation of harvested yield of 2021 with 2018 temperatures

As can be seen, there is an increase in production of about 15%, arriving at absolute values comparable to the average production of the different years, while there is no difference in the percentage of radiation at which the decrease in production is detected.

A similar simulation was done by inserting instead the temperature values of the year 2021 into the year 2019, to see if this had resulted, as in the previous simulation, in a production drop, but if this had also affected the percentage of shading at which the drop is detected [Fig. 6.21].

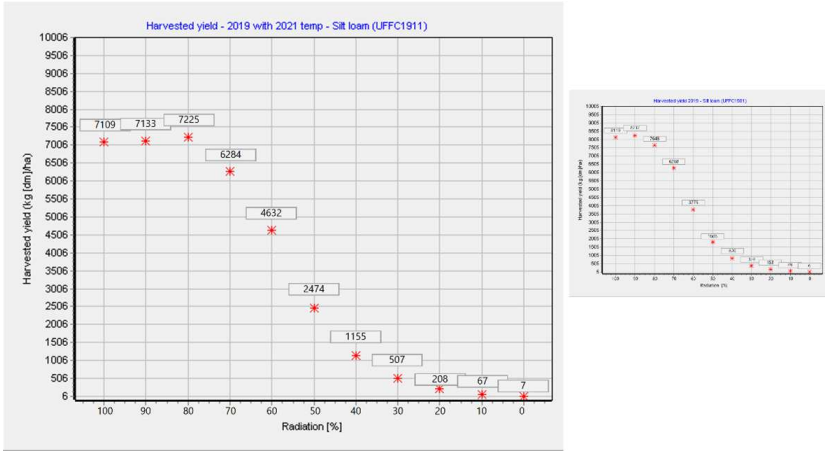

Figure 6.21: Simulation of harvested yield of 2019 with 2021 temperatures

A production decline of about 12% is observed in Fig. 6.21, and there is also a little shift in the percentage at which the production decline is detected, from 80% to 70%. A similar simulation was done by entering 2018 temperature values into 2019 to see if this affected absolute yield and crop profile as shading changed [Fig. 6.22].

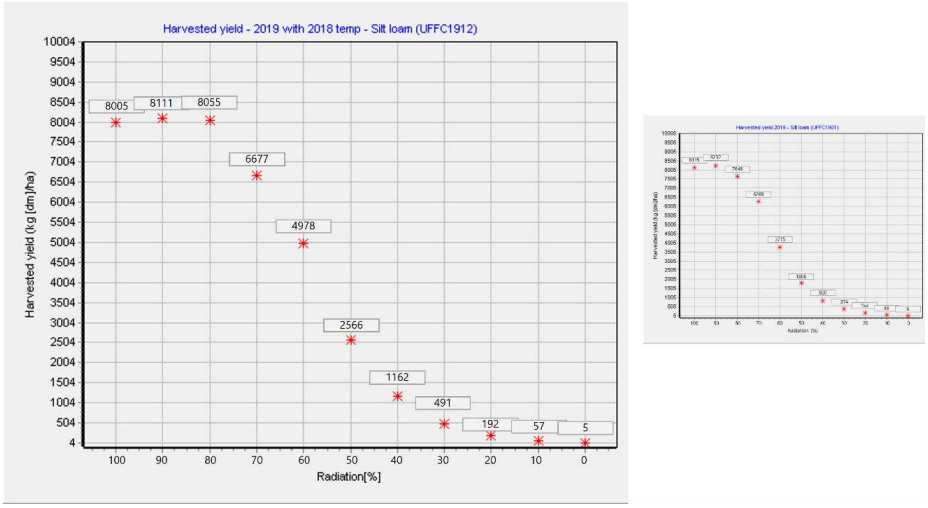

Figure 6.22: Simulation of harvested yield of 2019 with 2018 temperatures

From Fig. 6.22 it can be seen that the same conclusions obtained in the simulation of Fig. 6.21 can be drawn.

Finally, a comparable simulation was also done considering the year 2022, which had, like 2021, rather low absolute harvest values but average radiation values [Fig. 6.23].

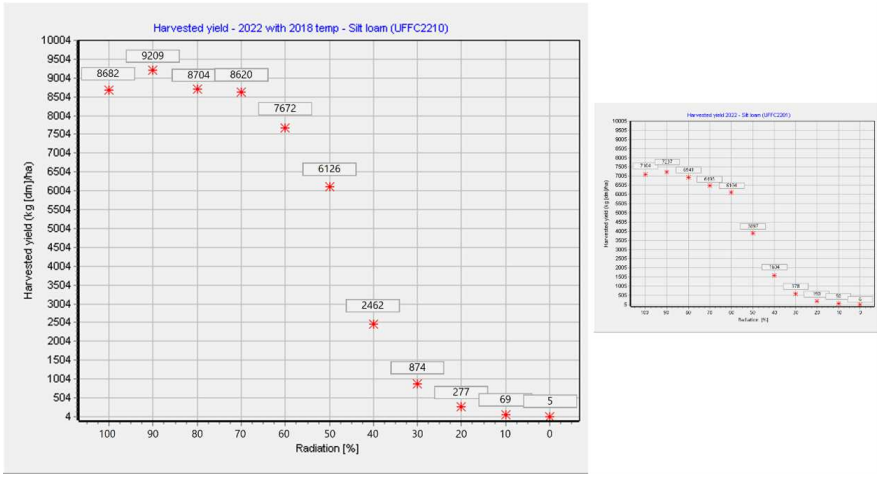

Figure 6.23: Simulation of harvested yield of 2022 with 2018 temperatures

Again, due to the increase in average temperatures to the 2018 level, there is an increase in absolute yield of about 22% and a slight increase in the amount of shading the crop can tolerate before experiencing a drop in yield, from 30 to 40%.

From these simulations, therefore, it can be said that temperature acts predominantly on absolute crop production and not on the percentage of shading at which production decline is detected, although it has been observed that this has minimal effect on the percentage of shading at which production decline occurs only in the case of years in which cumulative radiation is below average. Therefore, it can be said that this percentage is primarily affected by the percentage of incident radiation, as seen in section 6.3.1.

To summarize the relationship between radiation and temperature with respect to absolute production and the percentage of shading at which the production decline occurs, the two variables were correlated for of the first two months together [Fig. 6.24], which are the ones with the greatest variability for both variables.

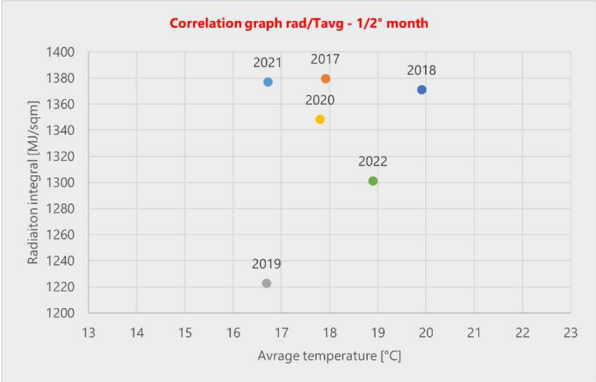

Figure 6.24: Correlation graph - Radiation integral and Average temperature in the first 2 months (2017-2022)

Thus, it can be seen from this graph that the percentage of shading is mainly determined by the incident radiation, as the years of lower irradiation (2019 and 2022) are those in which this production decreases to lower percentages (80 and 70% of the incident radiation, respectively). On the other hand, with regard to the effect of temperature on total production, this graph provides insights into some years such as 2021 and 2018 that have low and high production, respectively, 2017 and 2020 that have medium production, but less clearly explains years such as 2019 and 2022.

However, an explanation of these can be found if a third factor is considered, namely the influence of precipitation, as explained in section 6.3.3.

Note that the functionality of the environmental changes section of DSSAT was not used to explain the temperature increase in different years. In fact, that section allows only minimum and maximum temperatures to be changed and instead calculates an hourly average value of the mean temperature, which reflects a sinusoidal function as in Fig. 6.25.

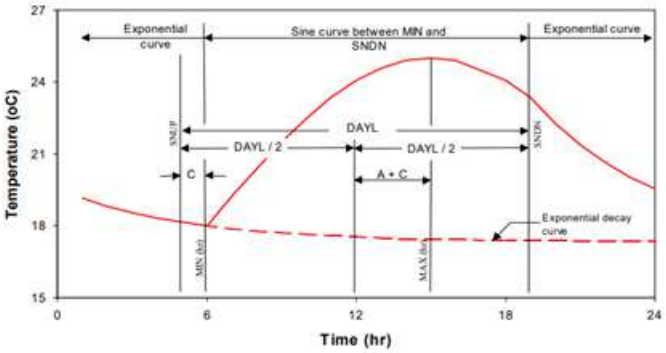

Figure 6.25: Daily Temperature Distribution calculated by DSSAT (Hoogenboom, 2010)

6.3.3 Precipitation

Precipitation was analyzed as the last parameter that could potentially have an effect on the final yield under the different panel shading scenarios.

As a first step, just as was done for incident radiation and temperature, rainfall trends over the years were studied for the crop months previously considered [Fig. 6.26].

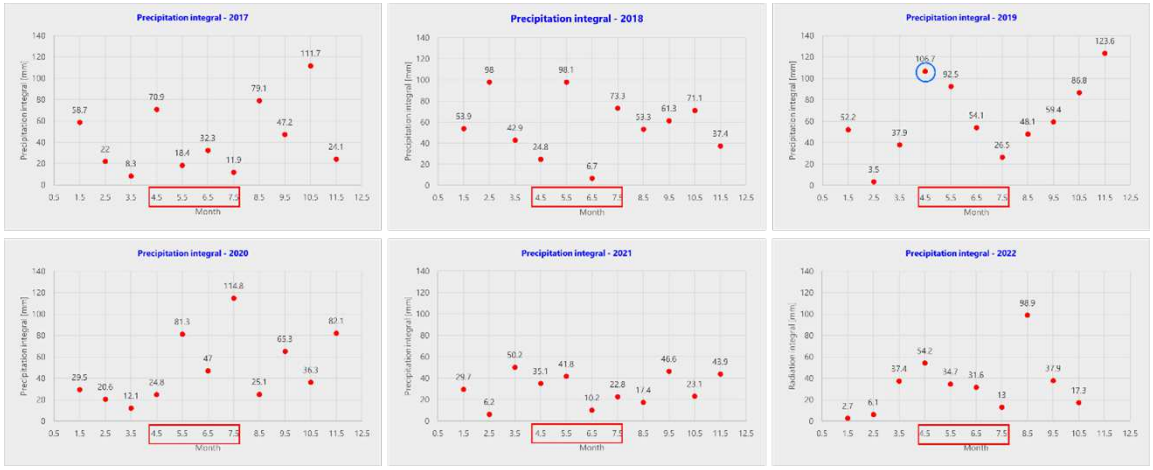

Figure 6.26: Monthly precipitation integral (2017-2022)

As can be seen from Fig. 6.26, precipitation varies quite significantly in the different months of the years considered, although it can be seen that the amount of precipitation in the first month of cultivation has always been in the range (24,70) mm, with the exception of 2019, which was a rather rainy year for all other months of interest. Note also how rainfall varies in the months preceding those in which potatoes are grown: for 2021 and 2022, these months recorded below-average rainfall values.

Regarding rainfall, two related effects can be evaluated: the effect of no rainfall and the effect of heavy rainfall. However, with regard to the former, it must be remembered, as mentioned in section 5.3.3, that the irrigation parameter was set in DSSAT as automatic, that is, the software

predicted irrigation of the soil when it fell below a threshold and exceeded a predetermined upper threshold of water in the soil (50 and 70%, respectively). Thus in the case of years with little precipitation, the software compensated for this low value by irrigating the soil, and the effect of little precipitation should in theory therefore not occur in the simulations. However, precipitation can go to affect more factors than just irrigation directly affecting soil water content, such as the temperature of the soil itself and the air above. Less precipitation, in fact, causes greater evaporation and consequent higher air humidity.

Therefore, to test the overall effect, and not only related to soil water content, of rainfall, the harvest of the year 2021, a particularly droughty year, was simulated again by imposing as rainfall that of the year 2018, a particularly rainy year with absolute production of the optimal crop, obtaining the results in Fig.6.27.

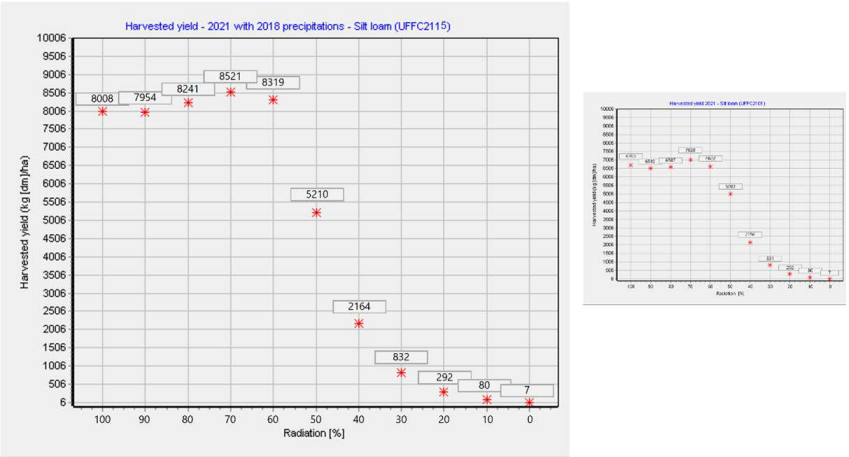

Figure 6.27: Harvested yield for 2021 with 2018 precipitations

As can be seen from Fig 6.27, the effect of shading remains unchanged from the actual year 2021, however, absolute production increases by 19.4%, thus becoming comparable to the average harvest in other years. For this reason, it can be assumed that rainfall does not go to affect the percentage of shading at which the production decline occurs, and therefore the presence of panels is not a problem for crop stability even in the case of drought years. The low rainfall, in fact, only goes to affect the absolute yield of the crop, regardless of the presence of the panels.

This result, however, was also obtained in the previous section [Fig. 6.20] by considering temperature as a critical variable. If one then combines the effects of the two, i.e., substituting 2021 for 2018 temperature and precipitation, one obtains [Fig. 6.28]:

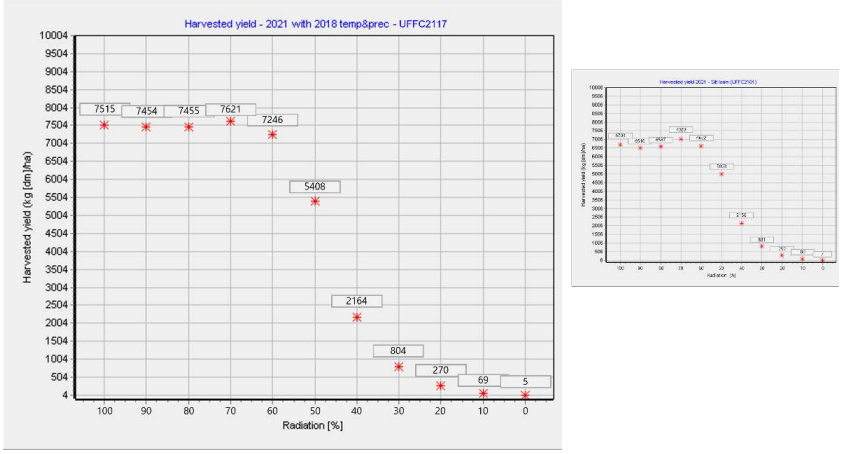

Figure 6.28: Harvested yield for 2021 with 2018 precipitations and temperatures

As can be seen from Fig 6.28, in this case the absolute yield is not equal to that seen above [Fig. 6.27], with a difference of about 6%, suggesting that the relationship between radiation, temperature, and precipitation, especially for years with intermediate climatic conditions, such as 2022, 2017, and 2020, is more complex and needs further investigation, including the distribution of these values over time. Indeed, this is also evident from the simulation for the year 2022, which also has average values of radiation and temperature, thus replacing the precipitation values of the year under consideration with the optimal values of 2018 [Fig. 6.29].

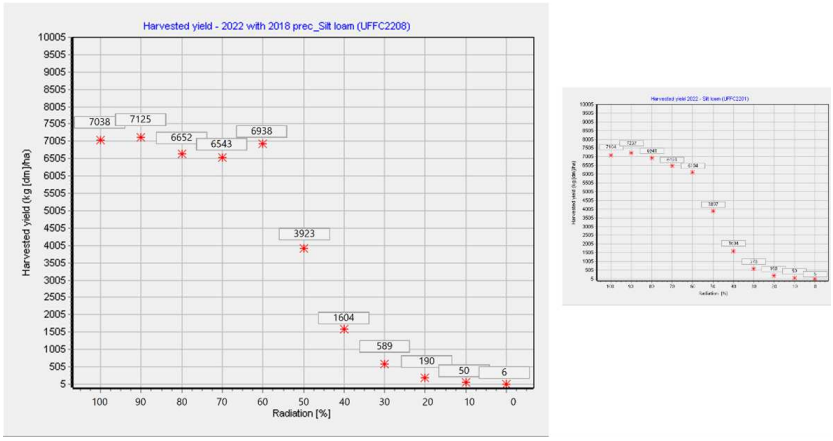

Figure 6.29: Harvested yield for 2022 with 2018 precipitations

In fact, increased rainfall results in a slight decrease in absolute yield, by about 1%, contrary to the linear hypothesis that increased rainfall could have a positive effect on overall final yield. However, again there was no decrease in yield with a different percentage of shading.

Therefore, to further verify that rainfall does not affect the percentage of shading at which the drop in production occurs, the same verification was carried out by replacing the rainfall in the year 2021 with that of the year 2019, a year in which the effect of shading is particularly pronounced. The result shown in Fig. 6.30 was obtained.

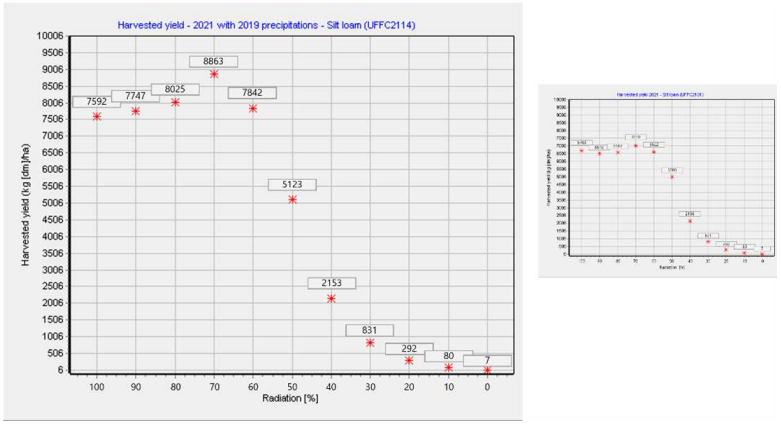

Figure 6.30: Harvested yield for 2021 with 2019 precipitations

As can be seen, the percentage of shading at which yield decline occurs remains unchanged, thus confirming that the lack of precipitation does not affect this factor, but only exclusively on absolute yield, in a nonlinear relationship with temperature and irradiance, however.

On the other hand, regarding the effect of abundance of precipitation on yield and shading, it was decided to evaluate its effect by imposing zero irrigation, in order to observe whether the percentage of shading at which the loss of radiation occurs was thus increased, thus being able to attribute the cause of the drop in production with shading to the abundant rainfall in the year considered, in addition to the incident radiation as previously observed.

Therefore, to study this case history, the year in which the incident radiation threshold in which the production decline occurred was lowest, i.e., 2019 (80% production decline), was taken as the reference, and zero irrigation was imposed [Fig. 6.31]. As mentioned above, 2019 was also the wettest of the six years considered.

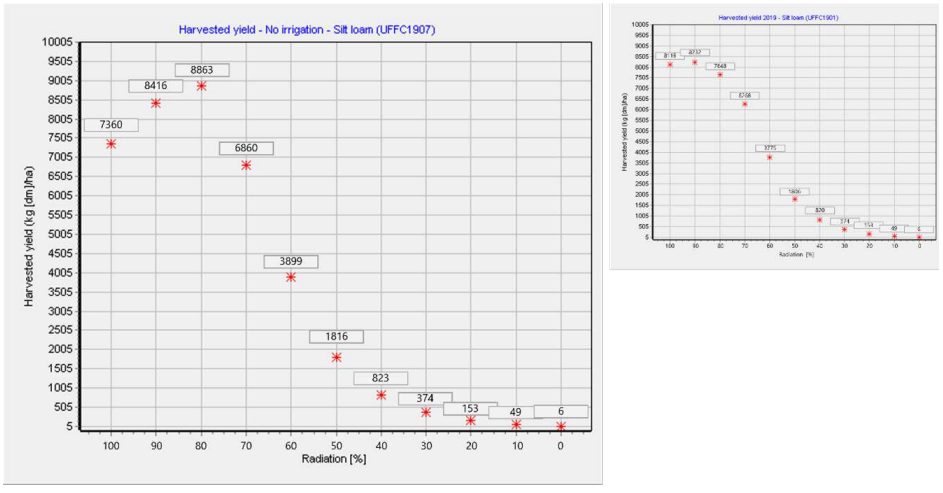

Figure 6.31: Simulation with no irrigation (2019)

As observed from Fig. 6.31, imposing zero irrigation did not result in a significant change in yield in all the shading levels. To ascertain this consideration, a one-tailed Mann-Whitney test was

performed, obtaining a U-value of 57. The critical value of U at $p < 0.05$ is 34. Therefore, the result is not significant at $p < 0.05$. The z-score is 0.197. The p-value is 0.42074. The result is not significant at $p < 0.05$. Thus, the two simulations are comparable, as expected.

As a further check, the amount of daily precipitation for the year was further reduced to equate it with the average of the other five years, under the assumption that the total precipitation was still high and the simple removal of irrigation was not sufficient to assess the effect. Daily precipitation values were then reduced by 39% so that they would be comparable to the average of about 42 mm, resulting in the simulation in Fig. 6.32.

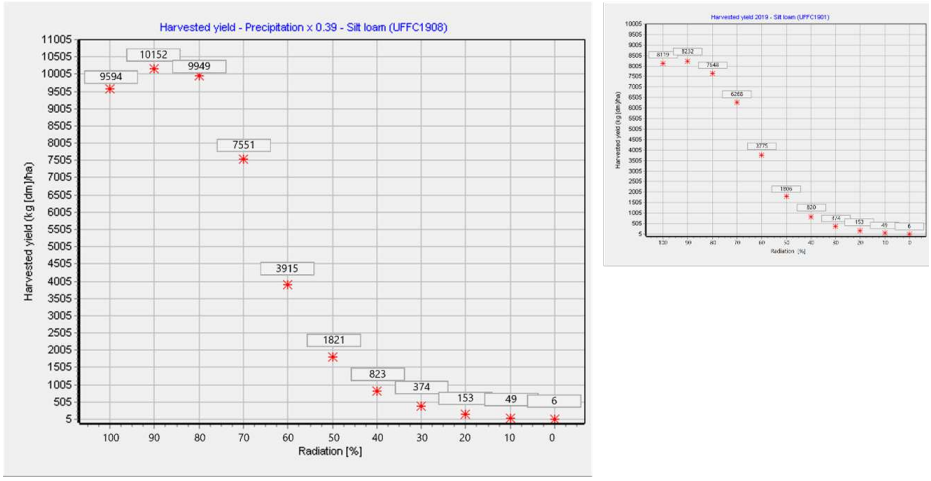

Figure 6.32: Simulation with precipitation reduction 0.39 (2019)

Again, the trend is very similar to that obtained in the normal scenario with 80% decay, and the two curves are comparable, with a U value of 54. The critical value of U at $p < 0.05$ is 34. Therefore, the result is not significant at $p < 0.05$. The z score is 0.39399. The p value is 0.34827. The result is not significant at $p < 0.05$.

From these results, it can be inferred that a higher rainfall rate has no effect on the percentage of incident radiation at which the loss of production occurs, and thus rainfall is not a determinant factor in this relative drop in production. Finally, note that in the simulation of Fig. 6.32, as rainfall decreases, there is a slight increase in absolute production, suggesting how the lower rainfall may benefit total production, even though it decreases the increase in absolute production that occurs at 80% incident radiation, which in fact goes from a 20% increase over the no-panel scenario in the simulation of Fig. 6.31 (without irrigation) to a 3.7% increase in the simulation of Fig. 6.32 (without irrigation). However, we defer the study of such detailed considerations of the effect of the absolute amount of rainfall on the potato crop and the relative increase in production in the presence of panels to later studies, as not of interest to this thesis work, where we focused primarily on the percentage of shading at which the production decline occurs.

6.4 Estimated yield in three agrivoltaic configurations

As mentioned before, after making the assessment of the reference soil on which to carry out the simulations, identifying the silt loam texture as optimal, analyzing the annual variation of the harvest, finding that the climatology of the six years used is comparable with the harvested yield obtained for the different years, and making a sensitivity study with respect to the response of the harvest to incident radiation, temperature and rainfall, the harvest output for three particular agrivoltaic configurations was to be simulated.

These configurations were taken as a reference downstream of optimization reasoning carried out in collaboration with the A2A company of the output and cost of the structures, which differed in three main parameters: the distance between rows of panels (pitch), the height of the panels, and the number of panels present (1P or 2P if one or two panels per module, respectively). Moreover, all configurations were based on trackers, i.e., sun-tracking structures. Thus, there were obtained two configurations with 2P trackers for a total width of 4.6 m width, 2 m standard height, and pitch at 10 and 14 m, and instead assuming a different agrivoltaic structure that is more present in the market, with 1P tracker structure of 2.4 m width with 4 m height and 5 m pitch panels.

To obtain a first approximation of the shading between rows of panels in these three structures, PVsyst software was used, assuming the cylinder of panel movement on tracker as in Fig. 6.33 through a series of simplifications such as considering the sail parallelepiped negligible. Indeed, PVsyst is a project design tool that allows the study, sizing and hourly simulation of photovoltaic plants.

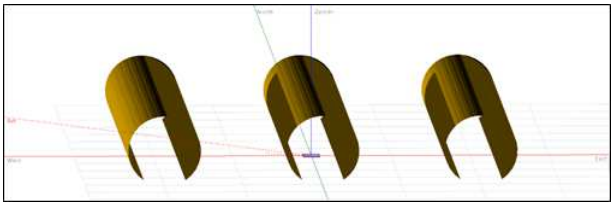

Figure 6.33: Panel movement on 2P tracker with 10 m pitch resulting in ground shading

From this model, the results in Tab. 6.2 of the radiation loss for different structures (distinct by pitch value, but with relative height and width characteristics as shown above) were then obtained.

Table 6.2: Soil samples summary

Measuring point [m]	Rad. pitch 10 m [%]	Rad. pitch 14 m [%]	Rad. pitch 5 m [%]
0.0	0.38	1.78	35.48
0.5	3.32	5.62	38.94
1.0	12.88	15.57	38.23
1.5	24.16	27.76	41.67
2.0	34.26	39.43	44.68
2.5	44.26	49.85	45.37
3.0	52.09	57.75	-
3.5	57.62	63.84	-
4.0	60.11	68.86	-
4.5	61.73	73.34	-
5.0	63.09	76.67	-
5.5	-	77.01	-
6.0	-	77.97	-
6.5	-	79.52	-
7.0	-	79.53	-

Then simulating such configurations on a silt loam plot and taking into consideration the six-year climatology yielded the following results [Fig. 6.34; 6.35; 6.36].

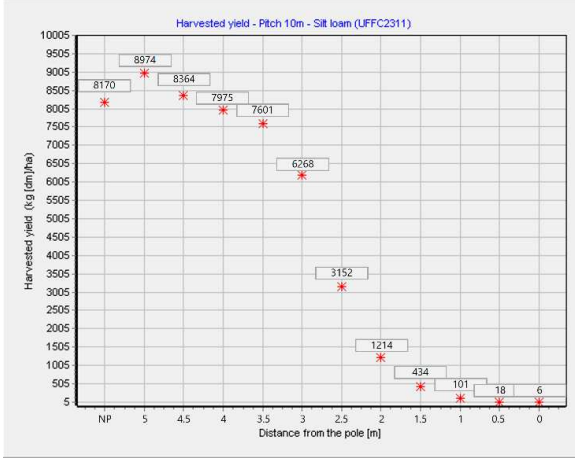

Figure 6.34: Harvested yield for an APV configuration with 10m pitch and standard height

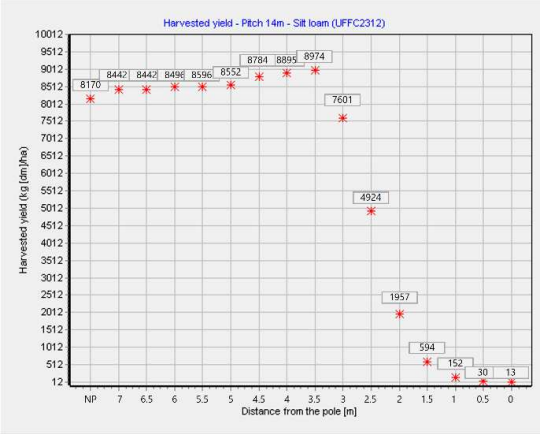

Figure 6.35: Harvested yield for an APV configuration with 14m pitch and standard height

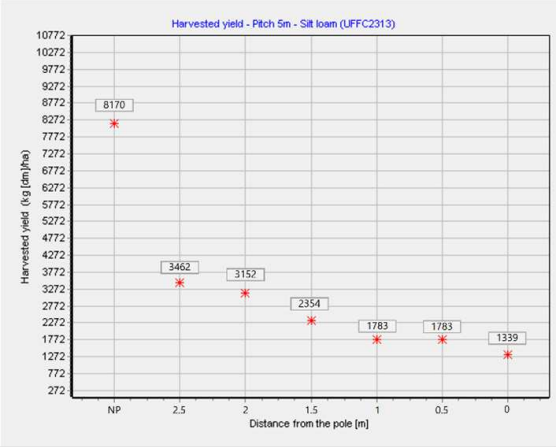

Figure 6.36: Harvested yield for an APV configuration with 5m pitch and 4m height

As can be seen from Fig. 6.36, the 5 m pitch configuration is not suitable for agrivoltaic application as there is a loss of 42% at the center of the rows, while the 10 m and 14 m pitch configurations both exhibit fairly constant yields up to 4 m and 3.5 m from the center of the panels, respectively, at which point for both configurations there is a production drop of about higher than 5%. Note that for the 14 m pitch agrivoltaic configuration, however, a slight increase due to the presence of the panels, of about 10%, occurs instead before the production drop, as seen for the initial simulation on silt loam at 70% and 60% incoming radiation [Fig. 6.2].

The choice between the two on the basis of crop yield falls to the 14 m pitch agrivoltaic configuration, since the 57% of the arable land between the rows does not see a decrease in production, compared to 20% for the 10 m pitch. However, the final choice also depends on reasoning of total power production versus total crop yield, which are deferred to future studies.

Chapter 7

Conclusions

This thesis work investigated the influence of the presence of photovoltaic panels, and their consequent shading on the soil, on the growth of the potato crop in the inter-row space of an agrivoltaic field.

The results obtained allow some conclusions to be drawn about the conditions of the soil on which potatoes are grown, the impact of weather variability on the annual crop, and especially which weather variables are most crucial in estimating the actual impact of the panels. These results were then used to simulate the impact of the panels for three different agrivoltaic configurations.

These analyses were carried out for potato cultivation on the Italian territory in the Emilia-Romagna province of Ferrara, and specifically for the Copparo area, where potato is most widespread regionally and where orographic conditions allow easy establishment of agrivoltaic configurations.

For that area, an assessment of initial conditions was first carried out. It was then simulated through the DSSAT software the harvest as the radiation decreases, which is the main environmental modification related to the presence of the panels, for four different soil types, categorized on the basis of texture and related soil data, keeping constant the crop management and meteorological data through the calculation of the climatology of the six years considered (2017-2022). From these simulations, it was found that for all the texture types identified in the area, the absolute harvest was consistent with the average harvest actually recorded in the Copparo area (amounting to about 40 $t \cdot ha^{-1}$), but the silt loam soil was selected as most representative, both in terms of suitability for potato cultivation and the number of samplings with a significant percentage of silt in the area.

Once the soil type was identified, the harvest was simulated for each of the six years 2017-2022 considered, both to verify the variation in harvest output based on annual weather variability and to confirm the validity of the climatology used in previous simulations. As a result, three different annual harvest categories emerged, characterized by the percentage of shading at which yield decline occurs, setting a 5% harvest difference between the no-panel scenario and the different shading scenarios as the threshold of significance. Specifically, 2019 was characterized by a production loss at the 20% shading level (thus corresponding to 80% incident radiation on the ground), 2017, 2020

and 2022 at the 30% level, and 2018 and 2021 at the 40% level. The representativeness of the climatology was then tested by comparing the yield obtained with one of the years whose distributions deviated the most, thus with a loss of production at low shading levels, such as 2019. The p-value obtained through the Mann-Whitney test was 0.206, thus above the significance threshold of 0.05, confirming that the two distributions are comparable, and therefore the climatology can be taken as a representative year of the six years considered.

Once this result was obtained, the analysis of the weather variability of the different years, and thus the resulting effect of photovoltaic panels on crops, was then entered into more detail. From the analysis of the impact of radiation over the years, it was found that the monthly variability of radiation over the growing season does not show a definite pattern when considering individual months, but instead the cumulative radiation of the first two to three months must be considered to fully understand the crop's response to shading.

To confirm this hypothesis derived from the graphical analysis of the data, several simulations were carried out in which panel shading was imposed for a single month, for the first two months, and for the first three months. For the first type of simulation, the first month in which the impact of shading was most significant was taken as the reference, obtaining p-values of the Mann-Whitney test for the different years all below the significance threshold of 0.05, in contrast to the p-values for the simulations with shading for the first two and three months. Thus, from this result, it can be concluded that there is an absolute value of incident radiation that must be achieved in the first two months for the crop to remain unaffected until 30-40% shading, within the range (1223,1301) $MJ \cdot sqm^{-1}$, and that therefore the yield decline in 2019 was due to the low radiation in the first two months, which did not exceed that minimum incident radiation threshold. However, since the software considered only the average daily radiation, it is suggested that this result should also be further investigated at the hourly level to further optimize future agrivoltaic configurations.

The years considered differed not only in response to shading but also in absolute production (i.e., in the scenario without panels), recording in fact years with little absolute harvest, such as 2021 and 2022, and years instead with high production, such as 2018. To understand the causes, and thus understand whether the addition of panels could have exacerbated these causes, the variation in temperature and precipitation over the years was studied.

Regarding temperature specifically, having ascertained that inhibition phenomena did not occur for any of the years considered, and taking 2018 as the optimal year for weather conditions as a reference, it was seen that for all the years with low production, the substitution of the 2018 temperature trend in the other years considered led to an increase in production. Specifically, both 2021 and 2022 saw increases of 15% and 20%, respectively, reaching absolute yield values comparable to the six-year average values. However, this increase in temperature did not significantly affect the percentage of shading at which the production decline is detected, thus arriving at the conclusion that the production loss with increasing shading is only due to the percentage of impacting radiation. In addition, a second result obtained from the temperature analysis is that the presence of photovoltaic panels, which it is hypothesized could lead to a slight increase in air temperature due to the creation of an underlying microclimate that has to be estimated in future studies, does not affect the absolute production drop in different years, but even could lead to an overall yield benefit for particularly cold years.

Finally, analyzing the precipitation variable, the effect of low precipitation on absolute yield and the percentage of shading at which yield decline occurs was also analyzed for this one. Regarding the latter, in none of the simulations was there a significant change in the percentage of irradiance at which the production drop occurs, thus being able to state that precipitation does not affect the production drop due to shading but radiation remains the only determining factor. On the other hand, with regard to the relationship between rainfall and total crop production, this is less evident than with temperature, both considering the increase in rainfall alone (e.g. for the

year 2022, which had an average high temperature, the average production level of the different years was not reached by raising rainfall, but rather there was a 1% decrease) and in relation to temperature (e. g. for 2021, raising both temperature and precipitation resulted in a lower increase in yield than that recorded by raising temperature and precipitation exclusively, a difference of about 6%). This confirms that the relationship between the three variables is not linear and needs to be further investigated in future studies to have a complete analysis on all the incident factors.

In addition, again with regard to precipitation, the opposite impact, which is that of excessive rainfall on the crop, was also investigated, taking 2019 as the reference year since it has rainfall about 39% above the average of other years. It was then found that excessive rainfall does not have impacts on the percentage of incident radiation at which production loss occurs, reconfirming the above, but exclusively on absolute production. In fact, reducing the 2019 precipitation by 39% to match the average of other years resulted in an increase in absolute production of about 18%. For this reason, too, a more detailed analysis of this relationship is deferred to future studies.

Finally, in light of the previous considerations, yields were simulated for three agrivoltaic configurations: 2P tracker with 10 m pitch and 14 m and standard 2 m height, and 1P tracker with 5 m pitch and 4 m height. These simulations showed that for the first two, the production drop occurs about 3-3.5 m from the center of the panels, with a production increase in the intrafila center of 10% for the 14 m pitch, suggesting this as the best agrivoltaic configuration. However, this result needs to be cross-referenced with trade-off reasoning between power production and total crop yield, which are deferred to future studies. This calculation should also take into account the entire crop rotation cycle, which was not the subject of this thesis work.

Therefore, from this thesis work, it can be concluded that, within the simulation limitations of the DSSAT software given by a variation of the radiation variable only daily and not hourly, the ideal agrivoltaic configuration should allow the potato crop to receive a certain threshold of incident radiation particularly in the first two months of their development period, to avoid having a production collapse with a low percentage of shading especially in particularly cloudy years (e.g. 2019). In addition, the agrivoltaic system does not affect the absolute yield, which is instead affected by factors such as temperature and rainfall in different years, but on the contrary, the hypothetical increase in temperature due to the microclimate that is assumed to be created under the photovoltaic panels, a hypothesis to be verified in more detail in future studies, could lead to an increase in yield, which would not occur in the absence of the system itself.

Chapter 8

Appendix

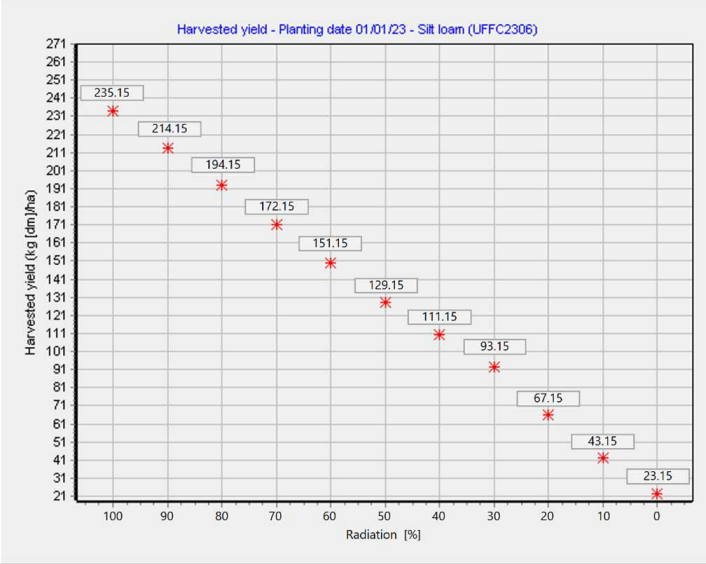

Figure 8.1: Planting date 01/01/23

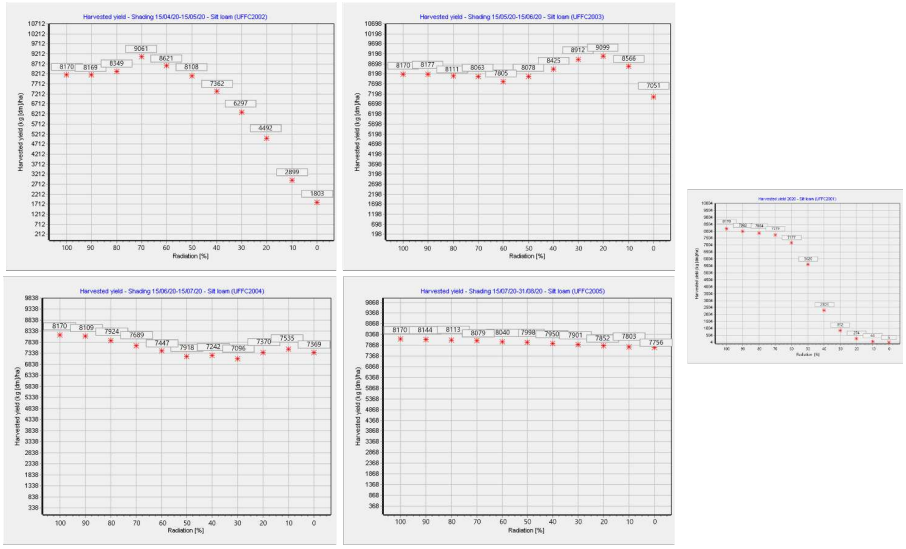

Figure 8.2: Harvested yield under monthly progressive shading scenarios (2020)

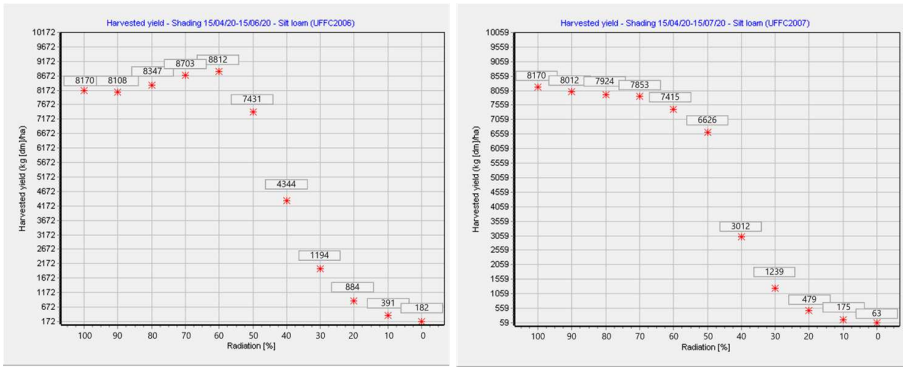

Figure 8.3: Simulations of the crop yield under shading of the first 2 months and the first 3 months (2020)

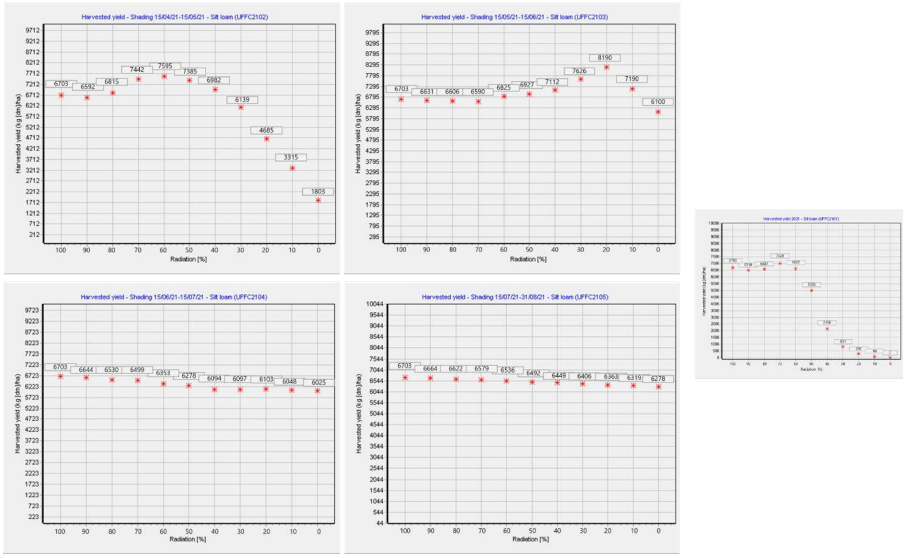

Figure 8.4: Harvested yield under monthly progressive shading scenarios (2021)

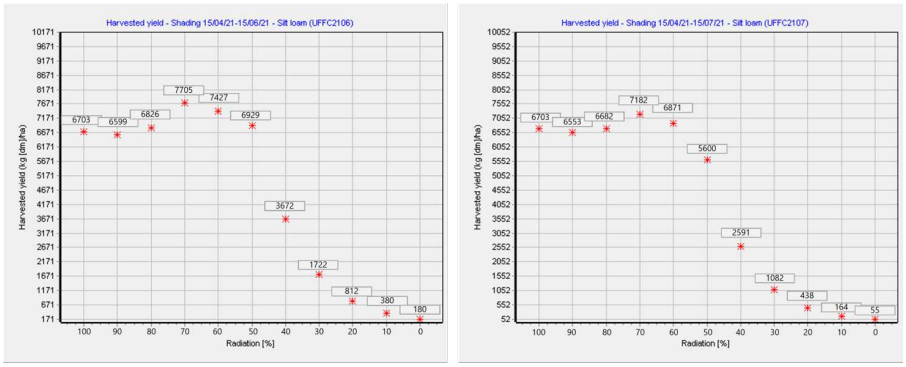

Figure 8.5: Simulations of the crop yield under shading of the first 2 months and the first 3 months (2021)

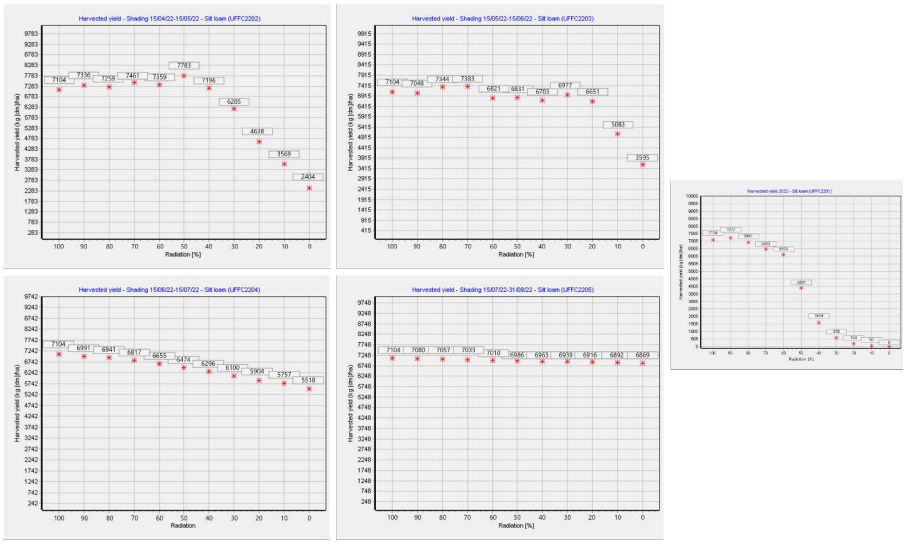

Figure 8.6: Harvested yield under monthly progressive shading scenarios (2022)

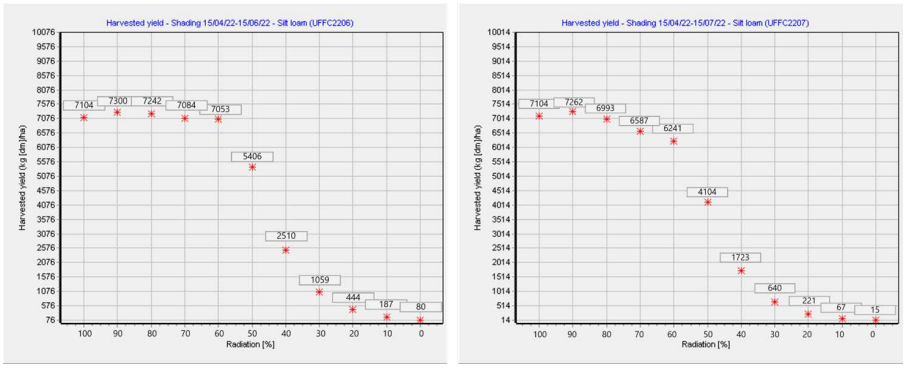

Figure 8.7: Simulations of the crop yield under shading of the first 2 months and the first 3 months (2022)

Chapter 9

References

A2A. (2022). *Discover our solar plants — A2A*. https://www.gruppoa2a.it/en/about-us/our-plants/solar

Adeh, E. H. (2019, August 7). Solar PV Power Potential is Greatest Over Croplands. *Nature.*

Agrivoltaics A Guideline for Germany. (2022). Fraunhofer ISE.

Ahmadi, S. H., Andersen, M. N., Plauborg, F., Poulsen, R. T., Jensen, C. R., Sepaskhah, A. R., Hansen, S. (2010). Effects of irrigation strategies and soils on field grown potatoes: Yield and water productivity. *Agricultural Water Management*, 97(11), 1923–1930. https://doi.org/10.1016/j.agwat.2010.07.007

Amaducci, S., Yin, X., Colauzzi, M. (2018). Agrivoltaic systems to optimise land use for electric energy production. *Applied Energy*, 220, 545–561. https://doi.org/10.1016/j.apenergy.2018.03.081

Antolini, G., Auteri, L., Pavan, V., Tomei, F., Tomozeiu, R., Marletto, V. (2015). A daily high-resolution gridded climatic data set for Emilia-Romagna, Italy, during 1961-2010. *International Journal of Climatology*, 36(4), 1970–1986. https://doi.org/10.1002/joc.4473

Antolini, G., Dottori, F. T. F., Marletto, V., Van Soetendael, M. (2015). Criteria banco di prova: Manuale Tecnico. *Area Agrometeorologia e Territorio del Servizio Idrometeorologico di Arpa Emilia-Romagna.*

Arsac. (2021, April 6). Arsac: guida ai principi di difesa integrata in agricoltura. *ARSAC Servizi in Agricoltura Calabria.*

Beck, M. (2012). Combining PV and Food Crops to Agrophotovoltaic? Optimization of Orientation and Harvest. *Proceedings of the 27th European Photovoltaic Solar Energy Conference and Exhibition.*

Bellini, E. (2020, June 8). Agrivoltaics works better with leafy greens, root crops. *PV Magazine International.*

CREA - Consiglio per la Ricerca in Agricoltura e l'analisi dell'Economia Agraria. (2021). *Redditività delle aziende agricole italiane.* https://rica.crea.gov.it/redditivita-31.php

CRITERIA - modello di bilancio idrico e sviluppo colturale. (n.d.). Arpae Emilia-Romagna.

Datta, S., Taghvaeian, S., Stivers, J. (2017). Understanding soil water content and thresholds for irrigation management. *Oklahoma Cooperative Extension Service.*

Disciplinari di produzione integrata - Norme tecniche per le colture orticole - Patata. (2022). Regione Emilia-Romagna.

Djaman, K., Koudahe, K., Koubodana, H. D., Saibou, A., Essah, S. (2022). Tillage Practices in Potato (Solanum tuberosum L.) Production: A Review. *American Journal of Potato Research*, 99(1), 1–12. https://doi.org/10.1007/s12230-021-09860-1

DSSAT Overview. (2022, January 7). *DSSAT.net.* https://dssat.net/about/

ERG5 - Dataset meteo orario e giornaliero dal 2001 - Dati Arpae. (n.d.). https://dati.arpae.it/dataset/erg5-interpolazione-su-griglia-di-dati-meteo

EU Parlament and Council. (2013). Regulation (EU) No. 1305/2013 on support for rural development by the European Agricultural Fund for Rural Development (EAFRD). https://eur-lex.europa.eu/legal-content/IT/TXT/?uri=celex:32013R1305

Food and Agriculture Organization (FAO). (n.d.). Annex 2 Infiltration rate and infiltration test. Retrieved December 1, 2022, from https://www.fao.org/3/s8684e/s8684e0a.htm

Food and Agriculture Organization of the United Nations (FAO) (n.d.). Potato - Land Water.

Geoportale 3D. (n.d.). Copyright(C) 2012-2022 Regione Emilia-Romagna, *National ICT Australia Limited (NICTA), CSIRO Data61. All Rights Reserved.* Retrieved August 1, 2021, from https://mappe.regione.emilia-romagna.it/

Giovannelli, V., Rastelli, V., Staiano, G. (2006). Quaderno Botanico agronomico: La patata. *Research Gate.*

Groenendyk, D. G., Ferré, T. P., Thorp, K. R., Rice, A. K. (2015). Hydrologic-Process-Based Soil Texture Classifications for Improved Visualization of Landscape Function. *PLOS ONE*, 10(6), e0131299. https://doi.org/10.1371/journal.pone.0131299

Hoogenboom, G., Wilkens, P. W., Tsuji, G. Y. (2010). DSSAT User's Guide Vol.4. https://dssat.net/wp-content/uploads/2011/10/DSSAT-vol4.pdf

Irriframe - il portale dell'irrigazione ANBI. (n.d.). https://www.irriframe.it/Irriframe

ISTAT. (2021). Coltivazioni - Ferrara. Retrieved August 24, 2022, from http://dati.istat.it/Index.aspx?DataSetCode=DCSP_COLTIVAZIONI

Italy's recovery and resilience plan. (2021). European Commission. Retrieved September 1, 2022, from https://bit.ly/3E4GBIj

Kapoor, S., Mahajan, B., Sharma, S., Gandhi, N. (2019). Storage behaviour of different potato varieties under ambient conditions. *Agricultural Research Journal*, 56(3), 576. https://doi.org/10.5958/2395-146x.2019.00090.5

Kincl, D., Kabelka, D., Vopravil, J., Heřmanovská, D. (2021). Estimating the curve number for conventional and soil conservation technologies using a rainfall simulator. *Soil and Water Research*, 16, 95–102. https://doi.org/10.17221/114/2020-SWR

Kuruppuarachchi, D. (1990). Intercropped potato (Solanum spp.): Effect of shade on growth and tuber yield in the northwestern regosol belt of Sri Lanka. *Field Crops Research*, 25(1–2), 61–72. https://doi.org/10.1016/0378-4290(90)90072-j

L'interpretazione delle analisi del terreno. (n.d.). Agenzia Regionale per La Prevenzione E Protezione Ambientale Del Veneto. https://www.arpa.veneto.it/arpavinforma/pubblicazioni/linterpretazione-delle-analisi-del-terreno

Markvart, T., Castañer, L. (2003). Practical handbook of photovoltaics: fundamentals and applications. *Elsevier EBooks.* https://cds.cern.ch/record/1084727/files/1856173909_TOC.pdf

McGee, E. (1986, December 1). The relationship between temperature and sprout growth in stored seed potatoes. *SpringerLink.*

Miller, D. E., Martin, M. W. (1983). Effect of daily irrigation rate and soil texture on yield and quality of Russet Burbank potatoes. *American Potato Journal*, 60(10), 745–757. https://doi.org/10.1007/bf02856894

Ministero dell'Economia e delle Finanze. (2021). Il Piano nazionale di Ripresa e Resilienza (PNRR). *Documentazione Parlamentare.*

Ministero della Transizione Ecologica. (2022). Impianti Agri-voltaici: pubblicate le Linee Guida — Ministero dell'Ambiente e della Sicurezza Energetica. https://www.mase.gov.it/notizie/impianti-agri-voltaici-pubblicate-le-linee-guida

Ministero delle Politiche Agricole e Forestali. (1999). Approvazione dei "Metodi ufficiali di analisi chimica del suolo": *Decreto ministeriale.* In https://www.gazzettaufficiale.it/eli/gu/1999/10/21/248/so/185/sg/pdf.

Owens, P. R., Rutledge, E. M. (2005). Encyclopedia of Soils in the Environment. *Elsevier.* https://www.sciencedirect.com/science/article/pii/B0123485304000023

Pavlista, A. D. (1995). Potato Production Stages: Scheduling Key Practices. *DigitalCommons University of Nebraska - Lincoln.* https://digitalcommons.unl.edu/extensionhist/1584/

Potato vegetative/generative growth balance. (2022, May 17). SQM Specialty Plant Nutrition.

Potenza, E. (2022). Agrivoltaic System and Modelling Simulation: A Case Study of Soybean (Glycine max L.) in Italy. *MDPI.* https://www.mdpi.com/2311-7524/8/12/1160

Reilly, J. (1996). Climate Change and Global Agriculture: Recent Findings and Issues on JSTOR. https://www.jstor.org/stable/1243242

Riserva idrica. (n.d.). Agenzia Regionale per La Prevenzione E Protezione Ambientale Del Veneto.

Russell, E. W., Paris, P. (1986). Il Terreno e la pianta: fondomenti di agronomia. Edagricole.

Schulz, V. S. (2019). Impact of Different Shading Levels on Growth, Yield and Quality of Potato (Solanum tuberosum L.). *MDPI.* https://www.mdpi.com/2073-4395/9/6/330

Staffilani, F. (2015). Carte Applicative - Carta dei Gruppi Idrologici della pianura emiliano-romagnola. *Geoportale 3D*

Staffilani, F. (2017). Carte Applicative - Carta della conducibilità idraulica satura dei suoli di pianura in scala 1:50.000. *Geoportale 3D.* Retrieved September 1, 2022.

Tarocco, P. (2021). Campioni Analisi Terreni (SACT) della Regione Emilia-Romagna (G. Sarno, Interviewer).

U.S. Department of Agriculture. (n.d.). USDA Soil Texture Calculator. Retrieved November 7, 2021

United States Department of Agriculture, U. (2022). National Engineering Handbook: Part 630 - Hydrology - Book 1. *Independently published.*

Woodward, D. E., Hawkins, R. H., Jiang, R., Hjelmfelt, Jr., A. T., Van Mullem, J. A., & Quan, Q. D. (2003). Runoff Curve Number Method: Examination of the Initial Abstraction Ratio. *World Water Amp;Amp; Environmental Resources Congress 2003.* https://doi.org/10.1061/40685(2003)308